https://doi.org/10.5194/acp-2019-1091
Preprint. Discussion started: 24 January 2020


Atmospheric Chemistry and Physics Discussions

# Seasonal impact of biogenic VSL bromine on the evolution of mid-latitude lowermost stratospheric ozone during the 21st century

Javier A. Barrera[1], Rafael P. Fernandez[1,2,3], Fernando Iglesias-Suarez[2], Carlos A. Cuevas[2], Jean-Francois Lamarque[4] and Alfonso Saiz-Lopez[2]

1 Institute for Interdisciplinary Science, National Research Council (ICB-CONICET), FCEN-UNCuyo, Mendoza, 5500, Argentina
[2] Department of Atmospheric Chemistry and Climate, Institute of Physical Chemistry Rocasolano, CSIC, Madrid, 28006, Spain
[3] Atmospheric and Environmental Studies Group (GEAA), UTN-FRM, Mendoza, 5500, Argentina
[4] Atmospheric Chemistry, Observations & Modelling Laboratory, National Center for Atmospheric Research, Boulder, CO 80301, USA

*Correspondence to*: Alfonso Saiz-Lopez & Rafael P. Fernandez (a.saiz@csic.es; rpfernandez@conicet.gob.ar)

**Abstract.** Biogenic very short-lived bromine ($VSL^{Br}$) represents, nowadays, ~25% of the total stratospheric bromine loading. Owing to their much shorter lifetime compared to anthropogenic long-lived bromine ($LL^{Br}$, e.g., halons) and chlorine ($LL^{Cl}$, e.g., chlorofluorocarbons) substances, the impact of $VSL^{Br}$ on ozone peaks at the extratropical lowermost stratosphere, a key climatic and radiative atmospheric region. Here we present a modelling study of the evolution of stratospheric ozone and its chemical losses in extra-polar regions during the 21st century, under two different scenarios: considering and neglecting the additional stratospheric injection of 5 ppt biogenic $VSL^{Br}$ naturally released from the ocean. Our analysis shows that the inclusion of $VSL^{Br}$ result in a realistic stratospheric bromine loading and improves the quantitative 1980–2015 model-satellite agreement of total ozone column (TOC) in the mid-latitudes. We show that the overall ozone response to $VSL^{Br}$ within the mid-latitudes follows the stratospheric abundances evolution of long-lived inorganic chlorine and bromine throughout the 21st century. Additional ozone losses due to $VSL^{Br}$ are maximised during the present-day period (1990-2010), with TOC differences of −8 DU (−3 %) and −5.5 DU (−2 %) for the southern (SH-ML) and northern (NH-ML) mid-latitudes, respectively. Moreover, the projected TOC differences at the end of the 21st century are at least half of the values found for the present-day period. In the tropics, a small (< –2.5 DU) and relatively constant (~ –1 %) ozone depletion mediated by VSL-bromine is closely related to its fixed emissions throughout the modelling period. We find that the seasonal $VSL^{Br}$ impacts on mid-latitude lowermost stratospheric ozone are influenced by the seasonality of the inorganic chlorine heterogeneous reactivation processes on ice-crystals. Indeed, due to the more efficient reactivation of chlorine reservoirs (mainly $ClONO_2$ and HCl) within the colder SH-ML lowermost stratosphere, the seasonal $VSL^{Br}$ impact shows a small but persistent hemispheric asymmetry through the whole modelling period. The largest modelled $VSL^{Br}$ impacts occur during the spring with local ozone changes during the present-day period of up to −10 % and −7 % at SH-ML and NH-ML, respectively. Our results indicate that, although the overall $VSL^{Br}$-driven ozone destruction is largest during the spring, the halogen-mediated ozone depletion ($Halog_{-Loss}$) in the mid-latitude lowermost stratosphere (~120 hPa) during the winter is comparatively more efficient than the HOx catalytic cycles respect to other seasons. Indeed, when $VSL^{Br}$ are considered, $Halog_{-Loss}$ dominates wintertime SH-ML lowermost stratospheric ozone losses between 1990 and 2020, with a contribution of inter-halogen $ClO_x$–$BrO_x$ cycles to $Halog_{-Loss}$ of approximately 50%. We conclude that considering

https://doi.org/10.5194/acp-2019-1091
Preprint. Discussion started: 24 January 2020


Atmospheric Chemistry and Physics Discussions

the coupling between biogenic bromine sources and seasonal changes of the chlorine heterogeneous reactivation are key features for future projections of mid-latitude lowermost stratospheric ozone during the 21st century.

## 1 Introduction

The role of bromine in stratospheric ozone depletion has been discussed in several studies (Wofsy et al., 1975; Prather and Watson, 1990; Daniel et al., 1999; Dvortsov et al., 1999; Solomon et al., 1999). Although bromine is much less abundant than chlorine in the atmosphere, it is known to deplete stratospheric ozone 45 to 69 times more efficiently on a per atom basis (Daniel et al., 1999; Sinnhuber et al., 2009). Moreover, the ozone depletion efficiency of active bromine (Br and BrO) is strongly related to the available amount of activated chlorine (manly Cl and ClO radicals) in the atmosphere (McElroy et al., 1986; Solomon et al., 1999, and references therein) as well as with enhanced sulfate aerosol loading, via heterogeneous reactions (Salawitch et al., 2005). Consequently, even low concentrations of bromine have a relatively large impact on stratospheric ozone. In addition to anthropogenic long-lived chlorine ($LL^{Cl}$) and bromine ($LL^{Br}$) substances, such as chlorofluorocarbons (CFCs), chlorocarbons, methyl bromide and bromofluorocarbons (halon fire suppressants), other substances with photochemical lifetimes shorter than 6 months, often referred to as very short–lived substances (VSL), have the potential to transport a significant amount of reactive halogens into the stratosphere. Owing to their short lifetimes, the impact of VSL on stratospheric ozone peaks at the extratopical lowermost stratosphere (Salawitch et al., 2005; Feng et al., 2007; Sinnhuber et al., 2009, 2015; Yang et al., 2014; Hossaini et al., 2015a; Falk et al., 2017) an important atmospheric region because surface temperature and climate are most sensitive to ozone perturbations (Riese et al., 2012; Hossaini et al., 2015b, Iglesias-Suarez et al., 2018). In fact, Hossaini et al. (2015b) found that very short-lived bromine ($VSL^{Br}$) exert a 3.6 times larger ozone radiative effect (normalized by halogen content) than that arising from long-lived substances. $VSL^{Br}$ are produced in the ocean, via the metabolism of marine organisms such as phytoplankton and macroalgae (e.g. Carpenter et al., 2007; Quack et al., 2007; Leedham Elvidge et al., 2015), even in sea-ice (e.g. Abrahamsson et al., 2018). Due to their high volatility, they are transferred into the marine boundary layer through air-sea exchange (Carpenter and Liss, 2000; Quack and Wallace, 2003). The most abundant $VSL^{Br}$ compounds released to the atmosphere are bromoform ($CHBr_3$) and dibromomethane (methylene dibromide, $CH_2Br_2$), followed by minor (but not-negligible) contribution of inter-halogen species (bromochloromethane, $CH_2BrCl$; dibromochloromethane, $CHBr_2Cl$ and bromodichloromethane, $CHBrCl_2$). Altogether, $VSL^{Br}$ contribute with ~ 5 (3–7) ppt to stratospheric bromine, which accounts for about 25% of total stratospheric bromine in 2016 (WMO, 2018). Moreover, this additional input of bromine is required to reconcile current stratospheric bromine trends (Salawitch et al., 2010; WMO, 2018).

Production of anthropogenic $LL^{Cl}$ and $LL^{Br}$ substances has been restricted by the Montreal Protocol and its subsequent amendments and adjustments (Solomon et al., 1999). After application, the stratospheric $LL^{Cl}$ and $LL^{Br}$ load has peaked at the end of the 20th century and is decreasing at a rate that depends on their respective atmospheric lives. This imply, for example, that hydrogen chloride (HCl) shows a long-term decrease at a rate of about 0.5 % $yr^{-1}$ in the middle stratosphere between 60ºN and 60ºS, while total stratospheric bromine decreases at a rate of about 0.75% $yr^{-1}$ from 2004 to 2014 (WMO 2018). Accordingly, stratospheric ozone is expected to recover from the effects of anthropogenic halogen-induced loss on a similar timescale, which is already detectable in the Antarctic and upper stratosphere (e.g. Solomon et al., 2016a; Chipperfield et al., 2017; Dhomse et al. 2018; Strahan

https://doi.org/10.5194/acp-2019-1091
Preprint. Discussion started: 24 January 2020


Atmospheric Chemistry and Physics Discussions

and Douglass, 2008, and references therein). The total stratospheric chlorine and bromine budget derived for 2016 were 3,290 ppt Cl and 19.6 ppt Br, respectively (WMO, 2018), and are expected to return to their 1980 values, an arbitrary reference date before the discovery of the Antarctic ozone hole, around the middle of this century (Dhomse et al. 2018). Although we still lack a scientific consensus with respect to the future evolution of $VSL^{Br}$ oceanic source strength and stratospheric injection (WMO, 2014; Lennartz et al., 2015; Ziska et al., 2017), the continuous decrease of $LL^{Br}$ leads to an increase in the relative $VSL^{Br}$ contribution to total stratospheric bromine into the future. Thus, understanding the role of natural $VSL^{Br}$ sources is key for chemistry-climate projections.

The impact of additional bromine is closely related to the heterogeneous chemistry of chlorine (Solomon et al., 1999; Salawitch et al., 2005; Müller, 2012). The influence of temperature and water vapour in the heterogeneous conversion processes of inorganic chlorine reservoirs (mostly HCl and $ClONO_2$) into active radicals on sulphate aerosols, has been reviewed elsewhere (e.g. Anderson et al., 2012, 2017; Drdla and Müller, 2012; Anderson and Clapp, 2018). In particular, Drdla and Müller (2012) highlighted that an increase in water vapour above background values would allow chlorine activation at higher temperatures than those observed in polar regions, which led to the hypothesis that chlorine reactivation and subsequent ozone loss could occur in the lower stratosphere at mid-latitudes during the summer (Robertrech et al., 2019). Indeed, the spatial and seasonal distributions of chlorine monoxide and chlorine nitrate in the monsoon regions provide indicators of heterogeneous chlorine processing in the tropical and subtropical lowermost stratosphere of the northern hemisphere (Solomon et al., 2016b). Moreover, heterogeneous chorine reactivation has also been observed on ice-particles in cirrus clouds located near the tropopause (Borrman et al., 1996, 1997; Solomon et al., 1997; Bregman et al, 2002; Thornton et al., 2003). The occurrence of cirrus clouds was reported in the lowermost stratosphere of northern high-mid latitudes (Spang et al., 2015), with summertime clouds located up to ~3 km (or 40–50 K of potential temperature) above the tropopause (Dressler, 2009). Also, von Hobe et al. (2011) suggested that cirrus ice particles at low temperatures may promote a significant activation of heterogeneous chlorine in the tropical upper troposphere lower stratosphere. Finally, satellite observations indicate that chlorine activation also occurs in the Antarctic and Arctic subvortex regions, where processed air dispersing from the decaying vortex in spring induces rapid changes in extravortex trace gas abundances (Santee et al., 2011).

Previous chemistry-climate modelling studies considering $VSL^{Br}$ chemistry mainly focused on improving the model vs. observed mid-latitude ozone trends at the end of the 20$^{th}$ century (Feng et al., 2007; Sinnhuber et al., 2009). More recently, Sinnhuber and Meul (2015) have shown a much larger ozone depletion over the lowermost stratosphere during the 1979–1995 period and a larger ozone increase during 1996–2005 period, in better agreement with observations, by including $VSL^{Br}$ sources. Moreover, Falk et al. (2017) have reported that the projected additional $VSL^{Br}$ impact on ozone at the end of the 21$^{st}$ century is reduced compared to present day. This result are in agreement with that of Yang et al. (2014), who performed time-slice simulations to address the sensitivity of stratospheric ozone to a speculative doubling of $VSL^{Br}$ sources under different $LL^{Cl}$ scenarios. However, neither of the previous studies had distinguished the ozone depleting contribution – including its seasonal variability– that arises from $VSL^{Br}$ respect to $LL^{Br}$ throughout the 21$^{st}$ century.

In this work, using the CAM-Chem model, we present a coupled chemistry-climate modelling study (i.e. with an interactive ocean) from 1960 to 2100 with and without the contribution from $VSL^{Br}$ sources. We focus on natural $VSL^{Br}$-driven impacts on the temporal evolution of extra-polar stratospheric ozone and total ozone column (TOC),

https://doi.org/10.5194/acp-2019-1091
Preprint. Discussion started: 24 January 2020


Atmospheric Chemistry and Physics Discussions

distinguishing both the long-term seasonal change and the resulting hemispheric asymmetries. Additionally, we present a timeline assessment of the individual contribution from anthropogenic ($LL^{Cl}$ and $LL^{Br}$) and biogenic ($VSL^{Br}$) sources to stratospheric halogen loading throughout the 21st century, recognizing also the $VSL^{Br}$ contribution to the overall halogen-catalysed ozone losses in mid-latitude lowermost stratosphere and tropical lower stratosphere. The layout of the paper is as follows: Section 2 resumes the main characteristics and configuration of the CAM-Chem model, as well as the complete set of measurements that are used for validation. Section 3 presents a quantitative model-observation comparison of both TOC and stratospheric chlorine and bromine loading, as well as discusses long-term seasonal impacts mediated by $VSL^{Br}$ on TOC and stratospheric ozone. The final concluding remarks are summarized in Section 4.

## 2 Methods

The Community Earth System Model (CESM; version 1.1.1), with the Community Atmospheric Model including interactive chemistry (CAM-Chem; version 4), (Lamarque et al., 2012; Tilmes et al., 2016) has been used to explore $VSL^{Br}$-driven stratospheric ozone loss on three latitude bands: southern hemisphere mid-latitudes (SH-ML) (60–35º S), Tropics (Trop)(25º S–25º N) and northern hemisphere mid-latitudes (NH-ML) (35–60º N). The model setup follows the Chemistry-Climate Model Initiative (CCMI) REFC2 configuration described in detail by Tilmes et al. (2016), with the exception that here we consider a constant geographically distributed and seasonally-dependent oceanic emissions of six bromocarbons ($VSL^{Br}$= $CHBr_3$, $CH_2Br_2$, $CH_2BrCl$, $CHBrCl_2$, $CHBr_2Cl$ and $CH_2IBr$) (Ordóñez et al., 2012). It is worth noting that this emission inventory is based on a monthly-varying satellite chl-a climatology, which allows introducing a complete seasonal cycle on the emission strength and spatial distribution of oceanic bromocarbons. A full description of the $VSL^{Br}$ mechanism in CAM-Chem, including both biogenic and anthropogenic sources, heterogeneous recycling reactions, dry and wet deposition, convective uplift and large-scale transport has been given elsewhere (Ordóñez et al., 2012; Fernandez et al., 2014). Monthly and seasonally varying zonally averaged distributions lower boundary conditions of long-lived chlorine ($LL^{Cl}$ = $CH_3Cl$, $CH_3CCl_3$, $CCl_4$, CFC–11, CFC–12, CFC–113, HCFC–22, CFC–114, CFC–115, HCFC–141b, HCFC–142b) and long–lived bromine ($LL^{Br}$ = $CH_3Br$, H–1301, H–1211, H–1202, and H–2402) were considered following the A1 halogenated ozone–depleting substances emissions scenario from WMO Ozone Assessment Report (2011), while surface concentrations of $CO_2$, $CH_4$, $H_2$ and $N_2O$ were specified following the moderate Representation Concentration Pathway 6.0 (RCP6.0) scenario (Meinshausen et al., 2011; Eyring et al., 2013). In order to avoid unnecessary uncertainties associated with the speculative evolution of $VSL^{Br}$ oceanic emissions into the future, we used a constant annual source strength for the whole modelled period (i.e., the Ordoñez et al. emissions inventory was replicated for all years between 1950 and 2100).

The CAM-Chem configuration used here extends from the surface to approximately 40 km (3.5 hPa in the upper stratosphere) with 26 levels and includes a horizontal resolution of 1.9º latitude by 2.5º longitude. The number of stratospheric levels changes depending on the latitudinal region: within the tropics, there are eight levels above the tropopause (~100 hPa), with a mean thickness of 1.25 km (15.5 hPa) for the lower stratospheric levels and 5.2 km (3.8 hPa) between the two highest levels; while for the mid-latitudes, the tropopause is located approximately at ~200 hPa, and up to 12 model stratospheric levels. To have a reasonable representation of the overall stratospheric circulation, the integrated momentum that would have been deposited above the model top is specified by an upper

https://doi.org/10.5194/acp-2019-1091
Preprint. Discussion started: 24 January 2020


Atmospheric Chemistry and Physics Discussions

boundary condition (Lamarque et al., 2008). A similar procedure is applied to the altitude-dependent photolysis rate computations, which include an upper boundary condition that considers the ozone column fraction prevailing above the model top. The current CAM-Chem version includes a non-orographic gravity wave scheme based on the inertia-gravity wave (IGW) parameterization, an internal computation of the quasi-biennial oscillation (QBO) and a CCMI-based implementation of stratospheric aerosol and surface area density (see Tilmes et al., 2016, for details). Moreover, this model configuration uses a fully coupled Earth System Model approach, i.e. the ocean and sea ice are explicitly computed.

Two independent experiments (each of them with three individual ensemble members only differing in their 1950 initial conditions) were performed from 1960 to 2100, considering a 10-year spin-up to allow for stratospheric circulation stabilisation (i.e. each simulation started in 1950). The baseline set-up ($run^{LL}$) considered only the halogen $LL^{Cl}$ and $LL^{Br}$ contribution from anthropogenic chlorofluorocarbons (CFCs), hydrochlorofluorocarbons (HCFCs), halons, methyl chloride and methyl bromide; while the second set of simulations included, in addition to the above anthropogenic sources, the background biogenic contribution from $VSL^{Br}$ oceanic sources ($run^{LL + VSL}$). Differences between these two experiments allow quantification of the overall impact of $VSL^{Br}$ sources on stratospheric ozone, as well as to determine their relative contributions to the halogen mediated catalytic ozone depleting families. In addition, from this analysis it is also possible to distinguish the contributions of both $LL^{Br}$ and $VSL^{Br}$ to the inorganic fraction of stratospheric bromine ($Br_y^{LL+VSL} = Br_y^{LL} + Br_y^{VSL} = Br + BrO + HBr + BrONO_2 + BrCl + HOBr + 2Br_2 + BrNO_2$), whereas the inorganic fraction of chlorine ($Cl_y^{LL} = ClO + Cl + HOCl + 2Cl_2O_2 + 2Cl_2 + OClO + HCl + ClONO_2 + BrCl + ClONO_2$) arises only from the degradation of $LL^{Cl}$ which is identical for both experiments.

For the case of vertical distributions and latitudinal variations, the zonal mean of the ensemble mean of each independent experiment ($run^{LL}$ and $run^{LL+VSL}$) was computed from the monthly output before processing the data, while a Lowess filter with a 0.2 fraction was applied to all long-term time series to smooth the data. Most of the figures and values within the text include geographically averaged quantities for present-day (defined here as the 1990–2010 mean, nominally year 2000) and the end of the 21st century (defined here as the 2080–2100 mean, nominally year 2100) periods over the latitudinal bands defined above. To highlight seasonal changes, we computed the average for the months of December-January-February (DJF), March-April-May (MAM), June-July- August and September-October-November (SON). Ozone loss trends due to $VSL^{Br}$ between 2000 and 2100 were calculated on the basis of the least squares linear trends, while the trend errors were estimated as twice the statistical deviation stemming from the least squares fit. Model results were compared with selected observational data sets to provide a basic evaluation of its performance. The total ozone column modelled between 1980 and 2015 was tested with observations from the Solar Backscatter Ultraviolet (SBUV) merged total ozone column data set (Frith et al., 2017), while the stratospheric inorganic halogen abundances were compared to: *i*) the reported $Br_y$ trend in the latest WMO Ozone Assessment Reports (WMO, 2014 and 2018), which shows changes in total $Br_y$ derived from BrO experimental observations between 1991 and 2012; and *ii*) the Microwave Limb Sounder (MLS) observations of the annual mean volume mixing ratio of HCl + ClO (Waters et al., 2006; Livesey et al., 2018), which provides a lower limit of the $Cl_y$ abundance in the stratosphere from 2005 to 2015.

https://doi.org/10.5194/acp-2019-1091
Preprint. Discussion started: 24 January 2020


Atmospheric Chemistry and Physics Discussions

## 3 Results and Discussion

### 3.1 Contribution of $LL^{Cl}$, $LL^{Br}$ and $VSL^{Br}$ to stratospheric inorganic halogen loading.

The evolution (1960−2100) of the modelled annual mean abundances of inorganic chlorine ($Cl_y$) and bromine ($Br_y$), as well as the $VSL^{Br}$ sources, in the global upper stratosphere (3.5 hPa) and the low stratosphere (50 hPa) at mid-latitudes and tropics, are shown in Fig.1. In addition, Figure 1 also includes global $Br_y$ trends reported in recent WMO reports (WMO, 2014 and 2018) and the MLS observations (HCl + ClO). Clearly, the temporal evolution of $Cl_y^{LL}$ and $Bry^{LL}$ show a pronounced peak at the end of the 20th century and beginning of the 21st century, respectively, after which the abundance of both halogens decline. Within the A1 halogen emission scenario considered in this work, the $Cl_y^{LL}$ abundance in our model returns to its past 1980 levels just before ~2060 in the global upper stratosphere, whereas the prevailing $Bry^{LL}$ abundance for year 1980 are not recovered even by the end of the 21st century (see Fig 1a). In comparison, the evolution of $Br_y^{VSL}$ abundances remains constant over time, resulting in an additional and time-independent fixed contribution of ~5 ppt total bromine injection, which leads to maximum global-upper stratosphere $Br_y^{LL+VSL}$ abundances of up to ~ 20.5 ppt at the beginning of the 21st century. This is in agreement with previous studies performed only for present-time conditions (Fernandez et al., 2014). Furthermore, note that the modelled global $Br_y^{LL+VSL}$ abundances are in good agreement with the observations within reported errors, highlighting the importance of considering the additional contribution from $VSL^{Br}$ to determine the overall evolution of stratospheric ozone during the 21$^{st}$ century.

In contrast to the global-upper stratosphere, $Br_y^{LL}$ abundances returns to 1980 levels before ~2080 and ~2050 for the mid-latitudes and tropics, respectively, while the $Cl_y^{LL}$ return date remains unaltered (see Fig 1b–d). Although within the tropical lower stratosphere there still prevails a small carbon-bonded organic fraction that has not been converted to the reactive inorganic form, the contribution from $VSL^{Br}$ to inorganic bromine also reaches ~5 pptv in the mid-latitude lower stratosphere. As the oceanic $VSL^{Br}$ emission remains fixed at their present-day values throughout the whole modelled period, the stratospheric source gas (organic) and product gas (inorganic) injection arising from $VSL^{Br}$ does not show a significant change between 2000 and 2100. Although the increase in convective transport moving into the future enhances $VSL^{Br}$ source gas injection, the RCP 6.0 scenario also represents an increase in OH concentration compared to present times, which fasten the $VSL^{Br}$ to $Br_y^{VSL}$ conversion (Falk et al., 2017).

The validation of inorganic chlorine with (HCl + ClO) MLS observations clearly shows a good model-satellite agreement, mainly in the upper stratosphere where most chlorine has already been photochemically converted to $Cl_y^{LL}$. Note also that the inter-annual variation of MLS observations at 50 hPa occurs mainly due to the chlorine heterogeneous reactivation, which can be influenced by the polar vortex dynamics at mid-latitudes (Dhomse et al. 2018). The slight underestimation of the modelled $Cl_y$ abundance within the tropics is partially due to the missing contribution of anthropogenic VSL chlorine species (i.e., Hossaini et al., 2015b, 2017) that has not been considered in this work. Moreover, although for most of the results in the mid-latitude lowermost stratosphere presented in Sections 3.3 to 3.5 we processed output at 120 hPa instead of 50 hPa, below 50 hPa the fractional conversion of organic chlorine to $Cl_y^{LL}$ is very small and thus the inferred HCl + ClO MLS data has a very large uncertainty, which prevents a reliable satellite-model inter-comparisons at lower altitudes (Santee et al. 2011).

The stratospheric $Bry^{VSL}$ injection remains constant during the whole modelling period, representing ~25 % of $Br_y^{LL+VSL}$ in the global-upper stratosphere for year 2000, and increasing to ~40 % by the end of the 21$^{st}$ century.

https://doi.org/10.5194/acp-2019-1091
Preprint. Discussion started: 24 January 2020


Atmospheric Chemistry and Physics Discussions

These results are in agreement with those reported by Fernandez et al. (2017). Due to the much shorter lifetimes of $VSL^{Br}$ with respect to $LL^{Br}$, the above contributions increase in the lower stratosphere. For example, the $Br_y^{VSL}$ relative contribution to $Br_y^{LL+VSL}$ for year 2000 represents ~30 % over the mid-latitudes and ~45 % in the tropics. Furthermore, within the mid-latitudes, $Br_y^{VSL}$ represents up to 45 % of $Br_y^{LL+VSL}$ both at the end of the 21st century and in the years prior to 1980, while in the tropics, $Br_y^{VSL}$ represents up to 65 % for these time periods. Consequently, these changes in the relative contribution of $VSL^{Br}$ to total inorganic bromine over time, region and altitude under different inorganic chlorine abundances, lead to relatively different ozone losses within the regions and altitude regimes, as described in detail below.

Figure 2 shows the annual zonal mean distribution of inorganic chlorine and bromine abundances, as well as the corresponding $ClO_x/Cl_y$ and $BrO_x/Br_y$ percentage ratios (black contour lines) for present-day. Note that the $ClO_x/Cl_y$ and $BrO_x/Br_y$ ratios reflect the changes in the contribution of the active chlorine ($ClO_x$=ClO + Cl + HOCl + $2Cl_2O_2$ + OClO + $2Cl_2$) and bromine ($BrO_x$= BrO + Br) fractions relative to their total inorganic abundances. Equivalent results are presented for the end of the 21st century period in the Supporting Information (see Fig. S1). In the lowermost stratosphere, the available inorganic fraction of both chlorine and bromine rapidly increase with altitude as halogen atoms are released by the photolysis and oxidation from all $LL^{Cl}$, $LL^{Br}$ and $VSL^{Br}$ species. In contrast, within the upper stratosphere no major changes on inorganic halogen abundances are observed since the conversion from their organic sources is nearly complete. Although our model shows a symmetric hemispheric distribution in stratospheric $Cl_y$ and $Br_y$ abundances, there is a marked difference in the $ClO_x/Cl_y$ ratio. A clear example is the fingerprints (located at 15ºN and ~100 hPa) corresponding to an enhancement in the $Cl_y$ species heterogeneous reactivation due to the transport processes during the Indian summer monsoon (Solomon et al., 2016b). In the same line, the higher ClOx/Cly values modelled over the SH-ML lowermost stratosphere compared to NH-ML are mainly due to the enhancement in the chlorine heterogeneous reactivation processes on ice-crystal (i.e., HCl and $ClONO_2$ reactivation) (Santee et al., 2011; Solomon et al., 1999, and references therein), influenced mainly by the proximity of the Antarctic polar vortex edge and the lower temperatures prevailing at high and mid-latitudes of the southern hemisphere (see Fig. S2). Additionally, the favourable conditions for isentropic exchange of young subtropical air with extremely old winter polar vortex air masses within the SH-ML (Spang et al. 2015; Rolf et al. 2015), could drive an additional chlorine heterogeneous reactivation and thus enhance hemispheric asymmetry. Moreover, the increase in the $ClO_x$ abundance and $ClO_x/Cl_y$ ratio is highest during winter and spring for both SH-ML and NH-ML, consistent with the seasonal changes of the lowermost stratospheric temperatures that affect chlorine reactivation on ice-crystals (see Fig. S3). In contrast, a symmetric hemispheric distribution of BrOx/$Br_y$ ratio is modelled over the mid-latitude lowermost stratosphere, associated with bromine heterogeneous reactivation on sulphate aerosols (i.e., HBr and $BrONO_2$ reactivation) (Solomon et al., 1999, and references therein), which show neither any hemispheric asymmetry nor seasonal changes in the reactivation processes (see Fig. S4). Thus, even when the inclusion of $VSL^{Br}$ sources increase the total stratospheric $Br_y$ abundance and therefore its active fraction ($BrO_x$), the $BrO_x/Br_y$ ratio remains unchanged in the stratosphere during the whole modelled period (see Figs. 2b,c and S1b,c), highlighting that this ratio is nearly independent of the total inorganic bromine abundance.

https://doi.org/10.5194/acp-2019-1091
Preprint. Discussion started: 24 January 2020


Atmospheric Chemistry and Physics Discussions

### 3.2 Impact of $VSL^{Br}$ on the evolution of total ozone column (TOC)

The temporal evolution (1960–2100) of the modelled annual mean TOC over mid-latitudes and tropics, along with merged SBUV TOC observations, is illustrated in Fig. 3. In addition, Table 1 shows the annual and seasonal mean values of the absolute and relative TOC differences (ΔTOC) between the $run^{LL}$ and $run^{LL+VSL}$ experiments for the present-day and the end of the 21st century periods, as well as the ΔTOC trends (% $dec^{-1}$) over the century. A list of interesting features can be observed by comparing the results of TOC over the different latitudinal bands: *i)* the constant emission of biogenic $VSL^{Br}$ sources, introduces a continuous reduction in TOC that exceeds the model ensemble variability between the experiments, improving the overall model-satellite agreement with exception of the tropics; *ii)* within the mid-latitudes, the additional ozone loss due to $VSL^{Br}$ peaks during the present-day period, coinciding with the temporal location of the TOC minima for both experiments and reaching a $\Delta TOC^{2000}$ of approximately −8 DU (~ −2.5 %) and −5.5 DU (~ −1.6 %) for the SH-ML and NH-ML, respectively (see Table 1); *iii)* $VSL^{Br}$ impacts on TOC by the end of the 21st century are at least half of the values found for the present-day, which are consistent with projected ΔTOC trends of 0.15 and 0.10 % $dec^{-1}$ for SH-ML and NH-ML, respectively; *iv)* smallest $VSL^{Br}$ impacts are observed within the tropics, where including $VSL^{Br}$ worsens the model-observations agreement observed for the $run^{LL}$ simulation. However, it is worth noting that here the TOC differences due to $VSL^{Br}$ are small and close to −1.5 DU (< −1 %) during practically the entire modelled period, with a maximum $\Delta TOC^{2000}$ reaching − 2.1 DU (< −1 %). This is in line with a projected ΔTOC trend of 0.03 % $dec^{-1}$. Even though the largest model bias compared to the SBUV data is observed in the tropics, the minimum TOC is shifted ~5 years earlier (i.e., to year 1995) for the $run^{LL+VSL}$ experiment, in agreement with observations. Overall, our model results show a much larger ozone loss efficiency due to $VSL^{Br}$ within the mid-latitudes compared to the tropics.

Here, the modelled mid-latitude ΔTOC due to $VSL^{Br}$ lies within the lower range of previous modelling studies over the 1960–2005 (Sinnhuber and Meul, 2015) and 1980–2005 (Feng et al., 2007) periods. Our lower impacts during recent past are expected, as for example the detailed treatment of $VSL^{Br}$ sources in Sinnhuber and Meul (2015) results in an additional $Br_y^{VSL}$ injection of 6 ppt $Br_y$, while in Feng et al. (2007) the model configurations included, in addition to an VSL tracer, the direct supply of tropospheric $Br_y$ as a lower condition. Furthermore, our results are in accord with the future projection trends in Falk et al. (2017), although their analysis on annual mean ozone loss due to $VSL^{Br}$ only focused on the late 21st century (2075–2100).

Figure 4 shows the temporal evolution (1960–2100) of the annual and seasonal ΔTOC between the experiments for the SH-ML, tropics and NH-ML. In addition, an analysis of ΔTOC as a function of latitude for present-day and the end of the 21st century periods is shown in Fig. 5. The inclusion of $VSL^{Br}$ leads to a continuous reduction of TOC at all latitudes, with a larger ozone destruction efficiency moving from the tropics to the high-latitudes. Moreover, note that the seasonal relatives ΔTOC between both periods are statistically significant (here defined as $p < 0.05$) only at the mid-latitudes (see dotted lines at the bottom of Fig. 5D). This highlights that the $VSL^{Br}$–driven ozone depletion efficiency changes significantly over the century, even though the contribution from $VSL^{Br}$ sources to bromine stratospheric injection remains constant. Since gas-phase and heterogeneous inter-halogen reactions involving both bromine and chlorine play a fundamental role in the stratospheric ozone loss (McElroy et al., 1986; Solomon et al., 1999; Salawitch et al., 2005), the VSL-bromine efficiency in ozone depletion is primarily linked to the temporal evolution of the background inorganic halogen abundance, which shows a continuous decline in the

https://doi.org/10.5194/acp-2019-1091
Preprint. Discussion started: 24 January 2020


Atmospheric Chemistry and Physics Discussions

course of the 21st century from its peak values observed during 2000 (see Figs. 1). This is in line with the suggested by Yang et al. (2014).

Largest mid-latitude TOC differences between experiments occur during the spring −when the maximum seasonal TOC levels are found− followed by the winter. Maximum springtime $\Delta TOC^{2000}$ reaches −10 DU (~ −3 %) and −7.7 DU (~ −2 %) for the SH-ML and NH-ML, respectively (see Table 1 and Fig. 4). In contrast, during summer and autumn, the maximum $\Delta TOC^{2000}$ remain below −6.8 (~ −2.4 %) and −4 DU (~−4.1 %) for the SH-ML and NH-ML, respectively. This is in line with the ozone loss mediated by $VSL^{Br}$ within the southern polar cap reported by Fernandez et al. (2017), whom showed a maximum ozone depletion of up to −15 DU (~ −14 % of TOC) during the October months at the beginning of the century. Moreover, as mentioned above, the projected seasonal $VSL^{Br}$ impact on TOC significantly decreases towards the end of the century, with springtime ΔTOC trends of up to 0.20 and 0.14 % $dec^{-1}$ for the SH-ML and NH-ML, respectively (see Table 1). In comparison, the projected ΔTOC trends for summer and autumn reach approximately 0.10 % $dec^{-1}$ at mid-latitudes. However, note also that the changes in the magnitudes of these seasonal ΔTOC trends are mainly attributed to a marked seasonal difference of ozone loss mediated by $VSL^{Br}$ during the period of highest background halogen abundance (i.e. present-day). These seasonal differences are reduced towards the end of the 21st century, due to the declining of the long-lived inorganic halogens abundance. In contrast to mid-latitudes, no significant changes in the TOC loss due to $VSL^{Br}$ is projected for the tropics, though the model captures a slightly major TOC depletion during the 1990s. Therefore, the $VSL^{Br}$-driven ozone depletion is less sensitive to background halogen abundances, introducing an almost constant impact that is in line with its fixed emissions considered throughout the whole modelling period.

### 3.3 $VSL^{Br}$ impact on the ozone vertical distributions.

Timeline analysis of the annual mean stratospheric ozone difference between the experiments as a function of altitude over the mid-latitudes and tropics, is presented in Fig. 6. The inclusion of $VSL^{Br}$ produces a reduction in ozone concentrations (i.e., $O_3(z)$ number densities) throughout most of the stratosphere during the whole modelling period. The deepest $O_3(z)$ reductions occur during the present-day period over the mid-latitude lowermost stratosphere, reaching ozone differences ($\Delta O_3(z)$) of up to −8 % (−0.25 $10^{12}$ molecule $cm^{-3}$) and −5 % (−0.14 $10^{12}$ molecule $cm^{-3}$) for the SH-ML and NH-ML, respectively. Above 50 hPa (~20 km), the $\Delta O_3(z)$ are practically constant at around −1% for all latitudes, which are linked to the lesser role played by VSL−bromine compared to catalytic ozone losses by hydrogen ($HO_x$= OH+$HO_2$) and nitrogen ($NO_x$= NO+$NO_2$) oxides, as well as by long-lived reactive halogens (Brasseur and Solomon, 2005; Salawitch et al., 2005; Müller, 2012).

Our modelled $\Delta O_3(z)$ latitudinal distribution is in agreement with those reported by Sinhuber and Meul et al. (2015) during the 1980–2005 period, with larger percentage ozone losses deepening around the mid−latitudes tropopause. In contrast, the $\Delta O_3(z)$ latitudinal distribution by the end of the 21st century period is at least half-folded with respect to present-time (see Fig. 6e), which is consistent with projected local $\Delta O_3(z)$ trends of up to 1 and 0.5 % $dec^{-1}$ over the SH-ML and NH-ML, respectively (see Fig.6f). In agreement with our results, although using a set of time-slice sensitivity simulations with a variable and speculative $VSL^{Br}$ contribution on different background stratospheric $Cl_y$ abundances, Yang et al. (2014) determined that $VSL^{Br}$ has a significantly larger ozone impact under a high stratospheric chlorine background than under a low chlorine background. Interestingly, deepest $O_3$ ($z$) reductions

https://doi.org/10.5194/acp-2019-1091
Preprint. Discussion started: 24 January 2020




are located at precisely the same altitudes where the ClOx/Cly ratio peak is modelled within the SH-ML lowermost stratosphere (see Fig 2), which explains the hemispheric asymmetry in the $VSL^{Br}$ impacts. This highlights that the enhancement in local ozone depletion mediated by $VSL^{Br}$ is largest under a context of highest background active chlorine abundance, since it provides an additional partner for chlorine species involved in the ozone depleting inter−halogen chemical reactions (e.g. $BrOx-ClOx_{-Loss}$, see Section 3.4).

Figure 7 shows the seasonal zonal mean distribution of the $\Delta O_3(z)$ during the present-day period. The corresponding $\Delta O_3(z)$ (% $dec^{-1}$) trends over the century, are shown in Fig. S5. The largest contributions to the annual mean ozone loss over the mid-latitude lowermost stratosphere correspond to spring, followed by the preceding winter and the posterior summer, with springtime $\Delta O_3(z)$ reaching up to −10 % and −7 % for the SH-ML and NH-ML, respectively (see Fig. 7b,d). These seasonal enhancements in local ozone depletion mediated by $VSL^{Br}$ are influenced by the seasonal changes of the chlorine heterogeneous reactivation processes on lowermost stratospheric ice-crystals, since the main bromine heterogeneous reactivation processes occurs on sulphate aerosols, and, therefore, lack of seasonal changes. Consequently, since the seasonal changes in ozone losses are maximized during the present−day period, the largest local $\Delta O_3(z)$ trends are also projected for spring and winter, with springtime $\Delta O_3(z)$ trends reaching up to 1.6 and 0.7 % for the SH-ML and NH-ML, respectively (see Fig. S5b,d).

Compared to the annual mean, springtime absolute $O_3(z)$ reductions are deepened over the first ~ 5 km above the tropopause along mid-latitudes during the present-day period. Whereas during the summer and autumn, these reductions are located at higher altitudes (between 2 and 5 km above the tropopause) and over a narrower geographic area, mainly over the NH-ML. Therefore, the VSL-bromine introduces seasonal changes not only in the overall ozone reduction, but also in its vertical distribution. Moreover, since seasonal $VSL^{Br}$ impacts persist until the end of the century, they could lead to significantly different seasonal perturbations on the radiative effects mediated by ozone. Future studies are needed to explore the potential $VSL^{Br}$ -mediated seasonal effects on atmosphere's radiative balance.

Near the tropical tropopause, the $O_3(z)$ reductions due to $VSL^{Br}$ are practically constant during the whole modelled period, with $\Delta O_3(z)$ of approximately −2% (−0.06 $10^{12}$ molecule $cm^{-3}$) at 50 hPa (see Fig. 6b). Even with an increase in the contribution of $Bry^{VSL}$ to $Br_y^{LL+VSL}$ of up to 65 % by the end of century −due to the implementation of the Montreal Protoco (WMO, 2014, 2018) and the fixed stratospheric $Bry^{VSL}$ injection (~ 4 ppt)– $\Delta O_3(z)$ changes in the tropical lower stratosphere are not significant over the century (see Fig. 6f). This is line with the impacts modelled on TOC. In contrast, within mid-latitudes, the seasonal $VSL^{Br}$ impacts on ozone significantly decrease over the century between 50 hPa and the tropopause (and its surroundings) (see Figs. 6f and S5a–d), even though the contribution from $Bry^{VSL}$ to $Br_y^{LL+VSL}$ increases towards the end of the century. Moreover, the projected seasonal and annual $\Delta O_3(z)$ trends peak precisely at the same altitudes where the modelled relative $\Delta O_3(z)$ are significant (see Figs. 6f and S5a–d). These result highlights the clear dependence of $VSL^{Br}$ impacts with the temporal evolution of background halogen abundances and the halogens heterogeneous reactivation processes, which in turn depend on the formation and distributions of ice-crystal and stratospheric sulphate aerosol surfaces. In fact, the projected impacts on the ozone vertical distribution at the end of the century are similar to those prevailing before 1980 for both SH-ML and NH-ML, since the background halogen abundances are similar between these periods. Thus, potential future changes in the lowermost stratospheric temperature (i.e. influencing in part the ice-crystal formation), geoengineering of climate via injection of stratospheric sulphate, as well as the formation and

https://doi.org/10.5194/acp-2019-1091
Preprint. Discussion started: 24 January 2020


Atmospheric Chemistry and Physics Discussions

distribution of stratospheric aerosol (e.g. future volcanic eruptions) will directly influence the processes of halogen heterogeneous reactivation and consequently the $VSL^{Br}$-driven ozone loss efficiency (Tilmes et al., 2008, 2012; Banerjee et al., 2016; Klobas et al., 2017; Heckendorn et al., 2009).

### 3.4 Changes in the long-term seasonal evolution of Halogen-driven ozone loss rate due to $VSL^{Br}$.

In order to determine the drivers controlling the different seasonal and hemispheric behaviour of the $VSL^{Br}$-driven ozone loss efficiency in the lowermost stratosphere, we compute the odd oxygen chemical loss for the different ozone-depleting families, including the oxygen ($O_{x–Loss}$), hydrogen ($HO_{x–Loss}$), nitrogen ($NO_{x–Loss}$), and halogen ($Halog_{–Loss} = BrO_{x–Loss} + ClO_{x–Loss} + ClOx{-}BrO_{x–Loss}$) contributions (Brasseur and Solomon, 2005; Saiz–Lopez et al., 2014). The odd oxygen loss rates equations for the ozone-depleting families considered in this work are presented in Table S1. The formalism used here is based on the catalytic cycles and chemical families defined in Brasseur and Solomon (2005).

Figure 8, shows the temporal evolution of the annual percentage contribution of each ozone-depleting family to total ozone loss rate over the SH–ML lowermost stratosphere (~120 hPa) for the $run^{LL}$ and $run^{LL+VSL}$ experiments, as well as the seasonal evolution of $HO_{x–Loss}$ and $Halog_{–Loss}$ contributions. The corresponding figures for the NH–ML lowermost stratosphere (~120 hPa) and tropical lower stratosphere (~50 hPa), are shown in Figs. S6 and S7, respectively. $Halog_{–Loss}$ represents the second most important contribution to total ozone loss rate after the $HO_{x–Loss}$ (~ 80 %) at the mid-latitude (see Figs. 8a and S7a), while within the tropics it represents the third family after the $HO_{x–Loss}$ and $NO_{x–Loss}$. This partially explains the smaller $VSL^{Br}$-driven ozone depletion modelled within the tropics (see Fig. S7a), as $Halog_{–Loss}$ represents at most 10% of the total ozone destruction over this region even for the $run^{LL+VSL}$ experiment. Moreover, the enhancement in the $Halog_{–Loss}$ contribution by including $VSL^{Br}$ is directly compensated by a decrease in the $HO_{x–Loss}$ within the mid-latitudes. For example, during the present-day, $Halog_{–Loss}$ in the SH-ML increases from 18 % for the $run^{LL}$ experiment to 25 % for $run^{LL+VSL}$ experiment, which is compensated by ~6 % reduction in the $HO_{x–Loss}$. In particular, the interaction between different catalytic ozone-depleting cycles involving OH and halogen radicals, as well as the influence of reactive halogens in altering the $OH/HO_2$ ratio, have been described elsewhere (Bloss et al., 2005; Saiz-Lopez and von Glasow, 2012).

Even though the additional seasonal ozone depletion due to $VSL^{Br}$ peaks during spring followed by winter over the mid-latitudes, the largest $Halog_{–Loss}$ contribution to the total ozone loss occurs in winter, presenting a much smaller contribution during the rest of the year (see Figs. 8b,c and S6b,c). Indeed, this marked seasonal behaviour prevails both, during boreal winter in the NH-ML and during the austral winter in the SH-ML. This is explained by considering the strong seasonality increase in the active chlorine abundance (i.e. driven by the heterogeneous reactivation on ice-crystals), as well as the winter decline of $HO_x$ oxide abundance (i.e driven by the decrease in solar radiation with respect to summertime). In fact, the enhancement in the $Halog_{–Loss}$ contribution due to $VSL^{Br}$ leads $Halog_{–Loss}$ to be the dominant ozone depleting family during winter between 1985 and 2020 within the SH–ML, surpassing in importance the role played by the otherwise dominant $HO_{x–Loss}$. In contrast, no seasonal variability of $Halog_{–Loss}$ contribution is modelled within the tropics, and thus the monthly $VSL^{Br}$ impact on ozone remains approximately constant during the whole modelling period around the annual mean.

Figure 9 shows the long-term evolution of pure $BrO_{x–Loss}$ and $ClO_{x–Loss}$, as well as crossed $ClO_x{-}BrO_{x–Loss}$ contributions to the $Halog_{–Loss}$ as a function of months and years over the SH-ML lowermost stratosphere (120 hPa)

https://doi.org/10.5194/acp-2019-1091
Preprint. Discussion started: 24 January 2020




for both experiments ($run^{LL+VSL}$ and $run^{LL}$). Equivalent results are presented for the NH-ML and tropics in Figs. S8 and S9, respectively. For any fixed year, the contribution of $BrO_{x–Loss}$ peaks during late summer and early autumn, while its minimum contribution occurs during the austral winter. In contrast, both the $ClO_{x–Loss}$ and crossed $ClO_x–BrO_{x–Loss}$ reach their maximum contribution during winter and early spring. Consequently, the inclusion of $VSL^{Br}$ increases $BrO_{x–Loss}$ throughout the year, while also increasing the crossed $ClO_x–BrO_{x–Loss}$ contribution but only during winter. This is at the expense of a decrease in the $ClO_{x–Loss}$ contribution. In addition, the $ClO_x–BrO_{x–Loss}$ contribution reaches up to 50 % by including $VSL^{Br}$ between 1990 and 2020, decreasing towards the end of the century as $Cl_y$ abundances decrease. Both, the decrease of $ClO_x–BrO_{x–Loss}$ and $ClO_{x–Loss}$ over time is offset by an increase in the $BrO_{x–Loss}$ contribution. Accordingly, the inclusion of $VSL^{Br}$ produces similar changes in the evolution of the contributions of each of the cycles composing the $Halog_{Loss}$ over the NH-ML, although the monthly $BrO_{x–Loss}$ contribution is greater compared to the SH-ML during the entire simulation (see Fig. S8).

In summary, during the months when the $Halog_{Loss}$ contribution to total ozone loss is comparatively lower within the mid-latitudes (i.e. summer and autumn), $Halog_{Loss}$ is almost entirely dominated by $BrO_{x–Loss}$, while in months when its contribution is highest, a transition from the $ClO_x–BrO_{x–Loss}$ contribution (~ 50 %) at the beginning of the century towards $BrO_{x–Loss}$ at the end of the century is modelled. This explains the lesser ozone depleting efficiency mediated by $VSL^{Br}$ into the future. Thus, the halog-driven ozone losses projected towards the end of the 21st century are mostly dominated by $BrO_{x–Loss}$, leading to a less marked seasonal $VSL^{Br}$ impact in accordance with the results modellated on both the ozone vertical distribution and the TOC. In the tropics, $BrO_{x–Loss}$ dominates $Halog_{–Loss}$ for practically the entire modelled period (see Fig. S9), regardless of season, while $ClO_{x–Loss}$ represents a maximum contribution of up to ~40% only during the end 20th century. Furthermore, unlike mid-latitudes, crossed $ClO_{x–}BrO_{x–Loss}$ has a negligible contribution to the tropical $Halog_{–Loss}$, showing that the $VSL^{Br}$–driven ozone loss efficiency is independent of changes in the background halogen abundance throughout the modelling period.

## 4 Conclusions

This study has explored the impact of $VSL^{Br}$ substances on the temporal evolution of stratospheric ozone both in the late 20th century and in the course of the 21st century over the mid-latitudes and tropics. The analysis compares two independent experiments, one of which considers only the anthropogenic $LL^{Cl}$ and $LL^{Br}$ sources contributions, while the other considers−in addition to long-lived sources− the contributions of $VSL^{Br}$ oceanic sources. We have evaluated annual and seasonal mean changes on the stratospheric ozone vertical distribution and TOC, as well as examined the projected ozone depletion ($\Delta O_3$ and $\Delta TOC$) trends (% $dec^{-1}$) over the century, under a scenario where both the relative contribution of $VSL^{Br}$ to total inorganic bromine and the background inorganic chlorine abundances shift towards the future. Finally, we have also assessed the long-term seasonal contribution changes of the halogen-mediated ozone losses ($Halog_{–Loss}$) due to VSL-bromine focused on the lowermost stratosphere, distinguishing the role of pure ($BrO_{x–Loss}$ and $ClO_{x–Loss}$), and crossed ($ClO_x–BrO_{x–Loss}$) cycles that compose $Halog_{–Loss}$. The results presented here highlight the importance of considering natural sources of halocarbons to determine the overall evolution of extra-polar stratospheric ozone during the 21st century.

Our analysis shows that the inclusion of $VSL^{Br}$ results in a realistic stratospheric bromine loading that improves the quantitative 1980–2015 model-satellite agreement of TOC in the mid-latitudes, highlighting the need to consider its additional natural emissions sources to determine the overall evolution of ozone during the 21st century.

https://doi.org/10.5194/acp-2019-1091
Preprint. Discussion started: 24 January 2020


Atmospheric Chemistry and Physics Discussions

Here, the $VSL^{Br}$ introduces a continuous reduction on TOC during the entire modelled period, with the largest TOC depletion occurring during the period of highest background halogen abundance ($\Delta TOC^{2000}$= −8 DU (−2.5 %) for SH-ML and −5.5 DU (−1.6 %) for NH-ML). In turn, a significant decrease of the impact towards the end of the 21st century over mid-latitudes is projected, with ΔTOC trends of 0.15 and 0.10 % $dec^{-1}$ for SH-ML and NH-ML, respectively. Even though the contribution of VSL-bromine to total stratospheric bromine reaches almost 50% by the end 21st of the century, our simulations show a statistically significant smaller $VSL^{Br}$ impact on lowermost stratospheric ozone as we move into the future. This result highlights that $VSL^{Br}$-driven ozone loss is closely linked to the temporal evolution of $LL^{Cl}$ and $LL^{Br}$ abundances regulated by the Montreal Protocol, as suggested by Yang et al. (2014). In the tropics, although our model captures a slightly greater TOC depletion associated with $VSL^{Br}$ during the 1990s, no significant change is projected by the end of the 21st century. Our results are in accordance with previous modelling studies that included natural bromocarbons and explored stratospheric ozone evolution in the recent past (Salawitch et al., 2005; Feng et al., 2007; Sinhuber et al., 2015), as well as by the end of the 21st century (Falk et al., 2017). However, unlike these previous works, we have performed six independent simulations from 1960 to 2100 with an explicit representation of VSL bromocarbons, including geographically distributed time-dependent $VSL^{Br}$ oceanic sources, resulting in an additional time-independent fixed contribution of ~ 5 ppt to the bromine stratospheric injection.

Within the mid-latitudes, the greatest TOC depletion associated with $VSL^{Br}$ corresponds to the spring months followed by winter. with maximum springtime $\Delta TOC^{2000}$ reaching −10 DU (~ −3 %) and −7.7 DU (~ −2 %) for SH-ML and NH-ML, respectively. We find that the inclusion of $VSL^{Br}$ leads to seasonal changes on the overall depth and vertical distribution of ozone in the lowermost stratosphere, which could result to different seasonal perturbations on the radioactive effects mediated by ozone. This seasonal enhancement in the local ozone loss mediated by $VSL^{Br}$ is strongly influenced by the seasonal changes in chlorine heterogeneous reactivation processes on ice crystals (mainly by the $ClONO_2$ and HCl recycling). In fact, the additional increase in the efficiency of these chlorine reactivation processes over the SH-ML lowermost stratosphere leads to modelled hemispheric asymmetry in the ozone reductions mediated by the $VSL^{Br}$. However, in light of the increasing growth in anthropogenic $VSL^{Cl}$ sources (Hossaini et al., 2015a, 2017), which could lead to an additional enhancement on lowermost stratospheric chlorine levels, further studies are required to include their contribution and assess the consequent impact on the ozone evolution during the 21st century.

Finally, the $Halog_{-Loss}$ contribution to total ozone loss rate peaks in winter over the mid-latitudes, with a much smaller contribution during the other seasons. By including $VSL^{Br}$, $Halog_{-Loss}$ dominates the wintertime ozone loss over SH-ML during the 1990–2020 period, surpassing in importance the role played by the otherwise dominant $HOx_{-Loss}$. During summer and autumn, when $VSL^{Br}$ -driven seasonal local ozone loss are relatively low, $Halog_{-Loss}$ is almost entirely dominated by $BrO_{x-Loss}$. Due to the expected decrease in $LL^{Cl}$ abundances, a transition from $ClO_x$–$BrO_{x-Loss}$ to $BrO_{x-Loss}$ during the course of the 21st century is projected, leading to a less marked seasonal $VSL^{Br}$ impact towards the end of the century. In the tropics, $BrO_{x-Loss}$ represents the dominant loss for practically the entire modelled period, and consequently, no seasonal variability is modelled.

https://doi.org/10.5194/acp-2019-1091
Preprint. Discussion started: 24 January 2020


Atmospheric Chemistry and Physics Discussions

## 5 Data availability.

Computing resources, support and data storage are provided and maintained by the Computational and Information System Laboratory from the National Center of Atmospheric Research (CISL, 2017). The code of the CAM-Chem model can be downloaded from the site (https://www2.acom.ucar.edu/gcm/cam-chem). Data that support the finding of this study can be downloaded from the AC2 webpage (https://ac2.iqfr.csic.es/en/publications).

## 6 Author Contributions

R.P.F and A.S-L. designed the climatic experiments. R.P.F and J.A.B configured and run all the simulations. J.A.B processed both the result of all simulations and the available satellite data used for validation. A.S-L., F.I-S and C.A.C provided additional feedback on geophysical processing and representation. J.A.B and R.P.F have mainly written the manuscript. All co-authors were involved in the discussion and iterations of the manuscript.

## 7 Competing interests.

The authors declare that they have no conflict of interest.

## 8 Acknowledgements

This study has been funded by the Agencia Nacional de Promoción Científica y Técnica (ANPCYT PICT-2016-0714, Argentina) and the European Research Council Executive Agency under the European Union´s Horizon 2020 Research and Innovation programme (Project 'ERC-2016-COG 726349 CLIMAHAL'). R.P.F and J.A.B. would like to thanks additional finantial support from CONICET, UNCuyo (SeCTyP M032/3853) and UTN (PID 4920-194/2018). A.S-L., C.A.C and F.I-S. are supported by the Consejo Superior de Investigaciones Científicas (CSIC) of Spain. We are very thankful to D. Kinnison for very helpful discussions and suggestions.

## 9 References

Anderson, J. G., Wilmouth, D. M., Smith, J. B., and Sayres, D. S.: UV Dosage Levels in Summer: Increased Risk of Ozone Loss from Convectively Injected Water Vapor, Science, 337, 835–839, https://doi.org/10.1126/science.1222978, 2012.

Anderson, J. G., Weisenstein, D. K., Bowman, K. P., Homeyer, C. R., Smith, J. B., Wilmouth, D. M., Sayres, D. S., Klobas, J. E., Leroy, S. S., Dykema, J. A., and Wofsy, S. C.: Stratospheric ozone over the United States in summer linked to observations of convection and temperature via chlorine and bromine catalysis, P. Natl. Acad. Sci. USA, 114, 4905–4913, https://doi.org/10.1073/pnas.1619318114, 2017.

Anderson, J. G. and Clapp, C. E.: Coupling free radical catalysis, climate change, and human health, Phys. Chem. Chem. Phys., 20, 10569–10587, https://doi.org/10.1039/C7CP08331A, 2018.

https://doi.org/10.5194/acp-2019-1091
Preprint. Discussion started: 24 January 2020




Abrahamsson, K., Granfors, A., Ahnoff, M., Cuevas, C. A., & Saiz-Lopez, A.: Organic bromine compounds produced in sea ice in Antarctic winter, Nat. Commun., 9, 5291–5302, https://doi.org/10.1038/s41467–018–07062–8, 2018.

Banerjee, A., Maycock, A. C., Archibald, A. T., Abraham, N. L., Telford, P., Braesicke, P., and Pyle, J. A.: Drivers of changes in stratospheric and tropospheric ozone between year 2000 and 2100, Atmos. Chem. Phys., 16, 2727–2746, https://doi.org/10.5194/acp–16–2727–2016, 2016.

Bloss, W. J., Lee, J. D., Johnson, G. P., Sommariva, R., Heard, D. E., Saiz-Lopez, A., Plane, J. M. C., McFiggans, G., Coe, H., Flynn, M., Williams, P., Rickard, A. R., and Fleming, Z. L.: Impact of halogen monoxide chemistry upon boundary layer OH and $HO_2$ concentrations at a coastal site, Geophys. Res. Lett., 32, L06814, https://doi.org/10.1029/2004GL022084, 2005.

Brasseur, G. and Solomon, S.: Aeronomy of the Middle Atmosphere: Chemistry and Physics of the Stratosphere and Mesosphere, 3rd Editio., Springer, Dordrecht, The Netherlands, Chapter 5, 265–442, 2005.

Bregman, B., Wang, P. H., and Lelieveld, J.: Chemical ozone loss in the tropopause region on subvisible ice clouds, calculated with a chemistry-transport model, J. Geophys. Res., 107, 4032, https://doi.org/10.1029/2001JD000761, 2002.

Borrmann, S., Solomon, S., Dye, J. E., and Luo, B. P.: The potential of cirrus clouds for heterogeneous chlorine activation, Geophys. Res. Lett., 23, 2133–2136, https://doi.org/10.1029/96GL01957, 1996.

Borrmann, S., Solomon, S., Avallone, L., Toohey, D., and Baumgardner, D.: On the occurrence of ClO in cirrus clouds and volcanic aerosol in the tropopause region, Geophys. Res. Lett., 24, 2011–2014, https://doi.org/10.1029/97GL02053, 1997.

Carpenter, L. J. and Liss, P. S.: On temperate sources of bromoform and other reactive organic bromine gases, J. Geophy. Res., 105, 20539–20547, https://doi.org/10.1029/2000JD900242, 2000.

Carpenter, L. J., Wevill, D. J., Hopkins, J. R., Dunk, R. M., Jones, C. E., Hornsby, K. E., and McQuaid, J. B.: Bromoform in tropical Atlantic air from 25◦N to 25◦S, Geophys. Res. Lett., 34, L11810, https://doi.org/10.1029/2007GL029893, 2007.

Chipperfield, M. P., Bekki, S., Dhomse, S., Harris, N. R. P., Hassler, B., Hossaini, R., Steinbrecht, W., Thieblemont, R., and Weber, M.: Detecting recovery of the stratospheric ozone layer, Nature, 549, 211–218, https://doi.org/10.1038/nature23681, 2017.

CISL. (2017). Computational and Information Systems Laboratory. Cheyenne: HPE/SGI ICE XA System (NCAR Community Computing), Boulder, CO, USA. Boulder, CO, USA: National Center for Atmospheric Reserach (NCAR). https://doi.org/10.5065/D6RX99HX.

Daniel, J. S., Solomon, S., Portmann, R. W., and Garcia, R. R.: Stratospheric ozone destruction: The importance of bromine relative to chlorine, J. Geophys. Res., 104, 23871, https://doi.org/10.1029/1999JD900381, 1999.

https://doi.org/10.5194/acp-2019-1091
Preprint. Discussion started: 24 January 2020




Dessler, A. E.: Clouds and water vapor in the Northern Hemisphere summertime stratosphere, J. Geophys. Res., 114, D00H09, doi:10.1029/2009JD012075, 2009.

Dhomse, S. S., Kinnison, D., Chipperfield, M. P., Salawitch, R. J., Cionni, I., Hegglin, M. I., Abraham, N. L., Akiyoshi, H., Archibald, A. T., Bednarz, E. M.., Bekki, S., Braesicke, P., Butchart, N., Dameris, M., Deushi, M., Frith, S., Hardiman, S. C., Hassler, B., Horowitz, L. W., Hu, R.-M., Jöckel, P., Josse, B., Kirner, O., Kremser, S., Langematz, U., Lewis, J., Marchand, M., Lin, M., Mancini, E., Marécal, V., Michou, M., Morgenstern, O., O'Connor, F. M., Oman, L., Pitari, G., Plummer, D. A., Pyle, J. A., Revell, L. E., Rozanov, E., Schofield, R., Stenke, A., Stone, K., Sudo, K., Tilmes, S., Visioni, D., Yamashita, Y., y Zeng, G.: Estimates of ozone return dates from Chemistry-Climate Model Initiative simulations, Atmos. Chem. Phys., 18, 8409–8438, https://doi.org/10.5194/acp–18–8409–2018, 2018.

Dorf, M., Bösch, H., Butz, A., Camy-Peyret, C., Chipperfield, M. P., Engel, A., Goutail, F., Grunow, K., Hendrick, F., Hrechanyy, S., Naujokat, B., Pommereau, J.-P., Van Roozendael, M., Sioris, C., Stroh, F., Weidner, F., and Pfeilsticker, K.: Balloon-borne stratospheric BrO measurements: comparison with Envisat/SCIAMACHY BrO limb profiles, Atmos. Chem. Phys., 6, 2483–2501, https://doi.org/10.5194/acp–6–2483–2006, 2006.

Douglass, A., Stolarski, R. S., Schoeberl, M. R., Jackman, C. H., Gupta, M. L., Newman, P. A., Nielsen, J. E., and Fleming, E. L.: Relationship of loss, mean age of air and the distribution of CFCs to stratospheric circulation and implications for atmospheric lifetimes, J. Geophys. Res., 113, D14309, https://doi.org/10.1029/2007JD009575, 2008.

Drdla, K. and Müller, R.: Temperature thresholds for chlorine activation and ozone loss in the polar stratosphere, Ann. Geophys., 30, 1055–1073, https://doi.org/10.5194/angeo–30–1055–2012, 2012.

Dvortsov, V. L., Geller, M. A., Solomon, S., Schauffler, S. M., Atlas, E. L., Blake, D. R.: Rethinking reactive halogen budgets in the midlatitude lower stratosphere, Geophys. Res. Lett., 26, 1699–1702. https://doi.org/10.1029/1999GL900309. 1999.

Eyring, V., Lamarque, J.-F., Hess, P., Arfeuille, F., Bowman, K., Chipperfield, M. P., Duncan, B., Fiore, A., Gettelman, A., Giorgetta, M. A., Granier, C., Hegglin, M., Kinnison, D., Kunze, M., Langematz, U., Luo, B., Martin, R., Matthes, K., Newman, P. A., Peter, T., Robock, A., Ryerson, T., Saiz-Lopez, A., Salawitch, R., Schultz, M., Shepherd, T. G., Shindell, D., Stähelin, J., Tegtmeier, S., Thomason, L., Tilmes, S., Vernier, J.-P., Waugh, D. W. and Young, P. J.: Overview of IGAC/SPARC Chemistry-Climate Model Initiative (CCMI) Community Simulations in Support of Upcoming Ozone and Climate Assessments, SPARC Newsl., 40(January), 48–66, 2013.

Falk, S., Sinnhuber, B.-M., Krysztofiak, G., Jöckel, P., Graf, P., and Lennartz, S. T.: Brominated VSLS and their influence on ozone under a changing climate, Atmos. Chem. Phys., 17, 11313–11329, https://doi.org/10.5194/acp–17–11313–2017, 2017.

Feng, W., Chipperfield, M. P., Dorf, M., Pfeilsticker, K., and Ricaud, P.: Mid-latitude ozone changes: studies with a 3-D CTM forced by ERA-40 analyses, Atmos. Chem. Phys., 7, 2357–2369, https://doi.org/10.5194/acp–7–2357–2007, 2007

https://doi.org/10.5194/acp-2019-1091
Preprint. Discussion started: 24 January 2020




Fernandez, R. P., Salawitch, R. J., Kinnison, D. E., Lamarque, J.-F. and Saiz-Lopez, A.: Bromine partitioning in the tropical tropopause layer: implications for stratospheric injection, Atmos. Chem. Phys., 14, 13391–13410, https://doi.org/10.5194/acp–14–13391–2014, 2014.

Fernandez, R. P., Kinnison, D. E., Lamarque, J.–F., Tilmes, S. and Saiz-Lopez, A.: Impact of biogenic very short-lived bromine on the Antarctic ozone hole during the 21st century, Atmos. Chem. Phys., 17, 1673–1688, https://doi.org/10.5194/acp–2016–840, 2017.

Frith, S. M., Stolarski, R. S., Kramarova, N. A., and McPeters, R. D.: Estimating uncertainties in the SBUV Version 8.6 merged profile ozone data set, Atmos. Chem. Phys., 17, 14695–14707, https://doi.org/10.5194/acp–17–14695–2017, 2017.

Heckendorn, P., Weisenstein, D., Fueglistaler, S., Luo, B., Rozanov, E., Schraner, M., Thomason, L., and Peter, T.: The impact of geo-engineering aerosols on stratospheric temperature and ozone, Environ. Res. Lett., 4, 045108, https://doi.org/10.1088/1748–9326/4/4/045108, 2009.

Hendrick, F., M. Van Roozendael, M.P. Chipperfield, M. Dorf, F. Goutail, X. Yang, C. Fayt, C. Hermans, K. Pfeilsticker, J.P. Pommereau, J.A. Pyle, N. Theys, and M. De Mazière.: Retrieval of stratospheric and tropospheric BrO profiles and columns using ground-based zenith-sky DOAS observations at Harestua, 60° N, Atmos. Chem. Phys., 7, 4869–4885, https://doi.org/10.5194/acp–7–4869–2007, 2007.

Hendrick, F., Johnston, P. V., Kreher, K., Hermans, C., De Maziere, M., and Van Roozendael, M.: One decade trend analysis of stratospheric BrO over Harestua (60º N) and Lauder (44º S) reveals a decline, Geophys. Res. Lett., 35, L14801, https://doi.org/10.1029/2008GL034154, 2008.

Hossaini, R., Chipperfield, M. P., Saiz-Lopez, A., Harrison, J. J., von Glasow, R., Sommariva, R., Atlas, E., Navarro, M., Montzka, S. A., Feng, W., Dhomse, S., Harth, C., Mühle, J., Lunder, C., O'Doherty, S., Young, D., Reimann, S., Vollmer, M. K., Krummel, P. B., and Bernath, P. F.: Growth in stratospheric chlorine from short-lived chemicals not controlled by the Montreal Protocol, Geophys. Res. Lett., 42, 4573–4580, doi:10.1002/2015GL063783, 2015a.

Hossaini, R., M. P. Chipperfield, S. A. Montzka, A. Rap, S. Dhomse, and W. Feng.: Efficiency of short-lived halogens at influencing climate through depletion of stratospheric ozone, Nat. Geosci., 8, 186–190, https://doi.org/ 10.1038/NGEO2363, 2015b.

Hossaini, R., Chipperfield, M. P., Montzka, S. A., Leeson, A. A., Dhomse, S., and Pyle, J. A.: The increasing threat to stratospheric ozone from dichloromethane, Nat. Commun., 8, 15962, https://doi.org/10.1038/ncomms15962, 2017.

Iglesias-Suarez, F., Kinnison, D. E., Rap, A., Maycock, A. C., Wild, O., and Young, P. J.: Key drivers of ozone change and its radiative forcing over the 21st century, Atmos. Chem. Phys., 18, 6121–6139, https://doi.org/10.5194/acp–18–6121–2018, 2018.

Klobas, J. E., Wilmouth, D. M., Weisenstein, D. K., Anderson, J. G., & Salawitch, R. J.: Ozone depletion following future volcanic eruptions, Geophys. Res. Lett., 44, 7490–7499, https://doi.org/10.1002/2017GL073972, 2017.

https://doi.org/10.5194/acp-2019-1091
Preprint. Discussion started: 24 January 2020




Lamarque, J.-F., Kinnison, D. E., Hess, P. G., and Vitt, F. M.: Simulated lower stratospheric trends between 1970 and 2005: Identifying the role of climate and composition changes, J. Geophys. Res., 113, D12301, https://doi.org/10.1029/2007JD009277, 2008.

Lamarque, J.-F., Emmons, L. K., Hess, P. G., Kinnison, D. E., Tilmes, S., Vitt, F., Heald, C. L., Holland, E. A., Lauritzen, P. H., Neu, J., Orlando, J. J., Rasch, P. J. and Tyndall, G. K.: CAM-chem: description and evaluation of interactive atmospheric chemistry in the Community Earth System Model, Geosci. Model Dev., 5, 369–411, https://doi.org/10.5194/gmd–5–369–2012, 2012.

Leedham Elvidge, E. C., Oram, D. E., Laube, J. C., Baker, A. K., Montzka, S. A., Humphrey, S., O'Sullivan, D. A., and Brenninkmeijer, C. A. M.: Increasing concentrations of dichloromethane, $CH_2Cl_2$, inferred from CARIBIC air sam ples collected 1998–2012, Atmos. Chem. Phys., 15, 1939–1958, https://doi.org/10.5194/acp–15–1939–2015, 2015.

Lennartz, S.T., G. Krysztofiak, C.A. Marandino, B.M. Sinnhuber, S. Tegtmeier, F. Ziska, R. Hossaini, K. Krüger, S.A. Montzka, E. Atlas, D.E. Oram, T. Keber, H. Bönisch, and B. Quack.: Modelling marine emissions and atmospheric distributions of halocarbons and dimethyl sulfide: the influence of prescribed water concentration vs. prescribed emissions, Atmos. Chem. Phys., 15, 11753–11772, https://doi.org/10.5194/acp–15–11753–2015, 2015.

Livesey, N. J., Read, W. G., Wagner, P. A., Froidevaux, L., Lambert, A., Manney, G. L., F., L., Valle, M., Pumphrey, H. C., Santee, M. L., Schwartz, M. J., Wang, S., Fuller, R. A., Jarnot, R. F., Knosp, B. W., Martinez, E., and Lay, R. R.: Version 4.2x Level 2 data quality and description document, JPL D–33509, Rev. D., Jet Propulsion Lab, 2018.

McElroy, M. B., Salawitch, R. J., Wofsy, S. C., and Logan, J. A.: Reductions of Antarctic ozone due to synergistic interactions of chlorine and bromine, Nature, 321, 759–762, 1986.

Meinshausen, M., Smith, S. J., Calvin, K., Daniel, J. S., Kainuma, M. L. T., Lamarque, J. F., Matsumoto, K., Montzka, S. A., Raper, S. C. B., Riahi, K., Thomson, A., Velders, G. J. M., and Vuuren, D. P. P.: The RCP greenhouse gas concentrations and their extensions from 1765 to 2300, Clim. Change, 109, 213–241, https://doi.org/10.1007/s10584–011–0156–z, 2011.

Müller, R. Ed.: Stratospheric Ozone Depletion and Climate Change, RSC Publishing, Cambridge, Chapter 3, 78–99, 2012.

Ordóñez, C., Lamarque, J.-F., Tilmes, S., Kinnison, D. E., Atlas, E. L., Blake, D. R., Sousa Santos, G., Brasseur, G. and Saiz-Lopez, A.: Bromine and iodine chemistry in a global chemistry-climate model: description and evaluation of very short-lived oceanic sources, Atmos. Chem. Phys., 12, 1423–1447, https://doi.org/10.5194/acp–12–1423–2012, 2012.

Prather, M. J. and Watson, R. T.: Stratospheric ozone depletion and future levels of atmospheric chlorine and bromine, Nature, 344, 729–734, 1990.

Quack, B. and Wallace, D. W. R.: Air-sea flux of bromoform: Controls, rates, and implications, Global Biochem.



Cy., 17, 1023, https://doi.org/10.1029/2002GB001890, 2003.

Quack, B., Peeken, I., Petrick, G., and Nachtigall, K.: Oceanic distribution and sources of bromoform and dibromomethane in the Mauritanian upwelling, J. Geophys. Res., 112, C10006, https://doi.org/10.1029/2006JC003803, 2007.

Riese, M., Ploeger, F., Rap, A., Vogel, B., Konopka, P., Dameris, M., and Forster, P.: Impact of uncertainties in atmospheric mixing on simulated UTLS composition and related radiative effects, J. Geophys. Res. Atmos., 117, D16305, https://doi.org/10.1029/2012jd017751, 2012.

Robrecht, S., Vogel, B., Grooß, J.-U., Rosenlof, K., Thornberry, T., Rollins, A., Krämer, M., Christensen, L., and Müller, R.: Mechanism of ozone loss under enhanced water vapour conditions in the mid-latitude lower stratosphere in summer, Atmos. Chem. Phys., 19, 5805–5833, https://doi.org/10.5194/acp–19–5805–2019, 2019.

Rolf, C., Afchine, A., Bozem, H., Buchholz, B., Ebert, V., Guggenmoser, T., Hoor, P., Konopka, P., Kretschmer, E., Müller, S., Schlager, H., Spelten, N., Sumińska-Ebersoldt, O., Ungermann, J., Zahn, A., and Krämer, M.: Transport of Antarctic stratospheric strongly dehydrated air into the troposphere observed during the HALO-ESMVal campaign 2012, Atmos. Chem. Phys., 15, 9143–9158, https://doi.org/10.5194/acp–15–9143–2015, 2015.

Saiz-Lopez, A. and von Glasow, R.: Reactive halogen chemistry in the troposphere, Chem. Soc. Rev., 41, 6448–6472, https://doi.org/10.1039/c2cs35208g, 2012.

Saiz-Lopez, A., Fernandez, R. P., Ordóñez, C., Kinnison, D. E., Gómez Martín, J. C., Lamarque, J.-F., and Tilmes, S.: Iodine chemistry in the troposphere and its effect on ozone, Atmos. Chem. Phys., 14, 13119–13143, https://doi.org/10.5194/acp–14–13119–2014, 2014.

Salawitch, R. J., Weisenstein, D. K., Kovalenko, L. J., Sioris, C. E., Wennberg, P. O., Chance, K., Ko, M. K. W., and McLinden, C. A.: Sensitivity of ozone to bromine in the lower stratosphere, Geophys. Res. Lett., 32, L05811, https://doi.org/10.1029/2004GL021504, 2005.

Salawitch, R. J., Canty, T., Kurosu, T., Chance, K., Liang, Q., da Silva, A., Pawson, S., Nielsen, J. E., Rodriguez, J. M., Bhartia, P. K., Liu, X., Huey, L. G., Liao, J., Stickel, R. E., Tanner, D. J., Dibb, J. E., Simpson, W. R., Donohoue, D., Weinheimer, A., Flocke, F., Knapp, D., Montzka, D., Neuman, J. A., Nowak, J. B., Ryerson, T. B., Oltmans, S., Blake, D. R., Atlas, E. L., Kinnison, D. E., Tilmes, S., Pan, L. L., Hendrick, F., Van Roozendael, M., Kreher, K., Johnston, P. V., Gao, R. S., Johnson, B., Bui, T. P., Chen, G., Pierce, R. B., Crawford, J. H., and Jacob, D. J.: A new interpretation of total column BrO during Arctic spring, Geophys. Res. Lett., 37, L21805, https://doi.org/10.1029/2010GL043798, 2010.

Santee, M. L., Manney, G. L., Livesey, N. J., Froidevaux, L., Schwartz, M. J., and Read, W. G.: Trace gas evolution in the lowermost stratosphere from Aura Microwave Limb Sounder measurements, J. Geophys. Res., 116, D18306, https://doi.org/10.1029/2011JD015590, 2011.

Sinnhuber, B.-M., Sheode, N., Sinnhuber, M., Chipperfield, M. P., and Feng, W.: The contribution of



anthropogenic bromine emissions to past stratospheric ozone trends: a modelling study, Atmos. Chem. Phys., 9, 2863–2871, https://doi.org/10.5194/acp–9–2863–2009, 2009.

Sinnhuber, B.-M. and Meul, S.: Simulating the impact of emissions of brominated very short lived substances on past stratospheric ozone trends, Geophys. Res. Lett., 2449–2456, https://doi.org/10.1002/2014GL062975, 2015.

Solomon, S., Borrmann, S., Garcia, R. R., Portmann, R., Thomason, L., Poole, L. R., Winker, D., and McCormick, M. P.: Heterogeneous chlorine chemistry in the tropopause region, J. Geophys. Res., 102, 21411–21429, https://doi.org/10.1029/97JD01525, 1997.

Solomon, S.: Stratospheric ozone depletion: A review of concepts and history. Rev. Geosphys., 37, 275–316, https://doi.org/10.1029/1999RG900008, 1999.

Solomon, S., Ivy, D. J., Kinnison, D., Mills, M. J., Neely, R. R., and Schmidt, A.: Emergence of healing in the Antarctic ozone layer, Science, 353, 269–274, https://doi.org/10.1126/science.aae0061, 2016a.

Solomon, S., Kinnison, D., Garcia, R. R., Bandoro, J., Mills, M., Wilka, C., Neely III, R. R., Schmidt, A., Barnes, J. E., Vernier, J., and Höpfner, M.: Monsoon circulations and tropical heterogeneous chlorine chemistry in the stratosphere, Geophys. Res. Lett., 43, 12624–12633, https://doi.org/10.1002/2016GL071778, 2016b.

Spang, R., Günther, G., Riese, M., Hoffmann, L., Müller, R., and Griessbach, S.: Satellite observations of cirrus clouds in the Northern Hemisphere lowermost stratosphere, Atmos. Chem. Phys., 15, 927–950, https://doi.org/10.5194/acp–15–927–2015, 2015.

Strahan, S. E. and Douglass, A. R.: Decline in Antarctic Ozone Depletion and Lower Stratospheric Chlorine Determined From Aura Microwave Limb Sounder Observations, Geophys. Res. Lett., 45, 382–390, https://doi.org/10.1002/2017GL074830, 2018.

Tilmes, S., Müller, R., & Salawitch, R.: The sensitivity of polar ozone depletion to proposed geoengineering schemes, Science, 320, 1201–1204, https://doi.org/10.1126/science.1153966, 2008.

Tilmes, S., Kinnison, D. E., Garcia, R. R., Salawitch, R., Canty, T., Lee-Taylor, J., Madronich, S., and Chance, K.: Impact of very short-lived halogens on stratospheric ozone abundance and UV radiation in a geo-engineered atmosphere, Atmos. Chem. Phys., 12, 10945–10955, https://doi.org/10.5194/acp–12–10945–2012, 2012.

Tilmes, S., Lamarque, J., Emmons, L. K., Kinnison, D. E., Marsh, D., Garcia, R. R., Smith, A. K., Neely, R. R., Conley, A., Vitt, F., Martin, M. V., Tanimoto, H., Simpson, I., Blake, D. R. and Blake, N.: Representation of the Community Earth System Model ( CESM1 ) CAM4–chem within the Chemistry-Climate Model Initiative ( CCMI ), Geosci. Model Dev., 9, 1853–1890, https://doi.org/10.5194/gmd–9–1853–2016, 2016.

Thornton, B. F., Toohey, D. W., Avallone, L. M., Harder, H., Martinez, M., Simpas, J. B., Brune, W. H., and Avery, M. A.: In situ observations of ClO near the winter polar tropopause, J. Geophys. Res., 108, 8333, doi:10.1029/2002JD002839, 2003.

von Hobe, M., Grooß, J.-U., Günther, G., Konopka, P., Gensch, I., Krämer, M., Spelten, N., Afchine, A., Schiller, C., Ulanovsky, A., Sitnikov, N., Shur, G., Yushkov, V., Ravegnani, F., Cairo, F., Roiger, A., Voigt, C., Schlager,

https://doi.org/10.5194/acp-2019-1091
Preprint. Discussion started: 24 January 2020




H., Weigel, R., Frey, W., Borrmann, S., Müller, R., and Stroh, F.: Evidence for heterogeneous chlorine activation in the tropical UTLS, Atmos. Chem. Phys., 11, 241–256, https://doi.org/10.5194/acp–11–241–2011, 2011.

Waters, J. W., Froidevaux, L., Harwood, R. S., Jarnot, R. F., Pickett, H. M., Read, W. G., Siegel, P. H., Cofield, R. E., Filipiak, M. J., Flower, D. A., Holden, J. R., Lau, G. K., Livesey, N. J., Manney, G. L., Pumphrey, H. C., Santee, M. L., Wu, D. L., Cuddy, D. T., Lay, R. R., Loo, M. S., Perun, V. S., Schwartz, M. J., Stek, P. C., Thurstans, R. P., Boyles, M. A., Chandra, K. M., Chavez, M. C., Chen, G. S., Chudasama, B. V., Dodge, R., Fuller, R. A., Girard, M. A., Jiang, J. H., Jiang, Y., Knosp, B. W., Labelle, R. C., Lam, J. C., Lee, K. A., Miller, D., Oswald, J. E., Patel, N. C., Pukala, D. M., Quintero, O., Scaff, D. M., Van Snyder, W., Tope, M. C., Wagner, P. A., and Walch, M. J.: The Earth Observing System Microwave Limb Sounder (EOS MLS) on the Aura satellite, IEEE T, Geosci. Remote, 44, 1075–1092, https://doi.org/10.1109/TGRS.2006.873771, 2006.

World Meteorological Organization (WMO): Scientific Assessment of Ozone Depletion: 2010. Global Ozone Research and Monitoring Project-Report No. 52, Geneva, Switzerland, 2011.

World Meteorological Organization (WMO): Scientific Assessment of Ozone Depletion: 2014. Global Ozone Research and Monitoring Project-Report No. 55, Geneva, Switzerland, 2014.

World Meteorological Organization (WMO): Scientific Assessment of Ozone Depletion: 2018. Global Ozone Research and Monitoring Project-Report No. 58, Geneva, Switzerland, 2018.

Wofsy, S. C., McElroy, M. B., and Yung, Y. L.: The chemistry of atmospheric bromine, Geophys. Res. Lett., 2, 215–218, https://doi.org/10.1029/GL002i006p00215, 1975.

Yang, X., Abraham, N. L., Archibald, A. T., Braesicke, P., Keeble, J., Telford, P. J., Warwick, N. J., and Pyle, J. A.: How sensitive is the recovery of stratospheric ozone to changes in concentrations of very short-lived bromocarbons?, Atmos. Chem. Phys., 14, 10431–10438, https://doi.org/10.5194/acp–14–10431–2014, 2014.

Ziska, F., B. Quack, S. Tegtmeier, I. Stemmler, and K. Krüger.: Future emissions of marine halogenated very-short lived substances under climate change, J. Atmos. Chem., 74(2), 245–260, https://doi.org/10.1007/s10874–016–9355–3, 2017.

https://doi.org/10.5194/acp-2019-1091
Preprint. Discussion started: 24 January 2020


Atmospheric Chemistry and Physics Discussions

## 10 Tables and Figures

**Table 1: Annual and seasonal TOC changes (ΔTOC) mediated by $VSL^{Br}$ within the mid-latitudes and tropics during the present-day and the end of the 21st century periods, as well as the ΔTOC trends (% $dec^{-1}$) over century.**

| Season | Region | $\Delta TOC^{2000}$ [1] DU (%) | $\Delta TOC^{2100}$ [1] DU (%) | ΔTOC trends[2] (% $dec^{-1}$) |
|---|---|---|---|---|
| annual mean | NH-ML | – 5.5 ± 0.6 | –2.7 ± 0.2 | |
| | | (– 1.6 ± 0.6) | (– 0.8± 0.2) | 0.10 ± 0.03 |
| | Trop | – 2.1 ± 0.3 | – 1.5 ± 0.1 | |
| | | (– 0.8 ± 0.2) | (– 0.6 ± 0.1) | 0.03 ± 0.01 |
| | SH-ML | – 8.0 ± 0.8 | – 3.9 ± 0.4 | |
| | | (– 2.5 ± 0.3) | (– 1.2 ± 0.3) | 0.15 ± 0.04 |
| DJF | NH-ML | – 6.2 ± 0.1 | – 3.2 ± 0.3 | |
| | | (– 1.7 ± 0.6) | (– 0.8 ± 0.2) | 0.11 ± 0.03 |
| | Trop | – 2.3 ± 0.3 | – 1.8 ± 0.1 | |
| | | (– 0.9 ± 0.1) | (– 0.7 ± 0.1) | 0.02 ± 0.01 |
| | SH-ML | – 6.9 ± 0.6 | – 4.5 ± 0.2 | |
| | | (– 2.4 ± 0.4) | (– 1.5 ± 0.1) | 0.10 ± 0.03 |
| MAM | NH-ML | – 7.7 ± 0.9 | – 3.7 ± 0.3 | 0.14 ± 0.04 |
| | | (– 2.0 ± 0.6) | (– 0.9 ± 0.2) | |
| | Trop | – 2.1 ± 0.2 | – 1.5 ± 0.1 | 0.02 ± 0.01 |
| | | (– 0.8 ± 0.2) | (– 0.6 ± 0.1) | |
| | SH-ML | – 6.2 ± 0.5 | – 4.2 ± 0.2 | 0.11 ± 0.03 |
| | | (– 2.2 ± 0.3) | (– 1.4 ± 0.1) | |
| JJA | NH-ML | – 4.1 ± 0.6 | – 2.3 ± 0.2 | 0.09 ± 0.03 |
| | | (– 1.3 ± 0.2) | (– 0.7 ± 0.1) | |
| | Trop | – 2.0 ± 0.3 | – 1.6 ± 0.1 | 0.02 ± 0.01 |
| | | (– 0.8 ± 0.2) | (– 0.6 ± 0.1) | |
| | SH-ML | – 8.0 ± 0.9 | – 3.2 ± 0.4 | 0.19 ± 0.06 |
| | | (– 2.5 ± 0.2) | (– 0.9 ± 0.1) | |
| SON | NH-ML | – 3.8 ± 0.4 | – 1.6 ± 0.1 | 0.10 ± 0.03 |
| | | (–1.2 ± 0.1) | (– 0.5 ± 0.1) | |
| | Trop | –1.9 ± 0.2 | – 1.5 ± 0.1 | 0.01 ± 0.01 |
| | | (–0.7 ± 0.1) | (– 0.6 ± 0.1) | |
| | SH-ML | –10.0 ± 1.2 | – 5.7 ± 0.4 | 0.20 ± 0.06 |
| | | (–3.0 ± 0.8) | (– 1.6 ± 0.8) | |

[1] Absolute (DU) and relative (%, in brackets) TOC changes during the present-day ($\Delta TOC^{2000}$) and the end of the 21st century ($\Delta TOC^{2100}$) periods were computed considering the $run^{LL}$ and $run^{LL+VSL}$ experiments averaged within the mid-latitudes (SH-ML and NH-ML) and tropics (Trop). Annual and seasonal ΔTOC errors were estimated from standard errors of mean.

[2]Trend errors were estimated as twice the statistical deviation stemming from the least squares fit.

https://doi.org/10.5194/acp-2019-1091
Preprint. Discussion started: 24 January 2020


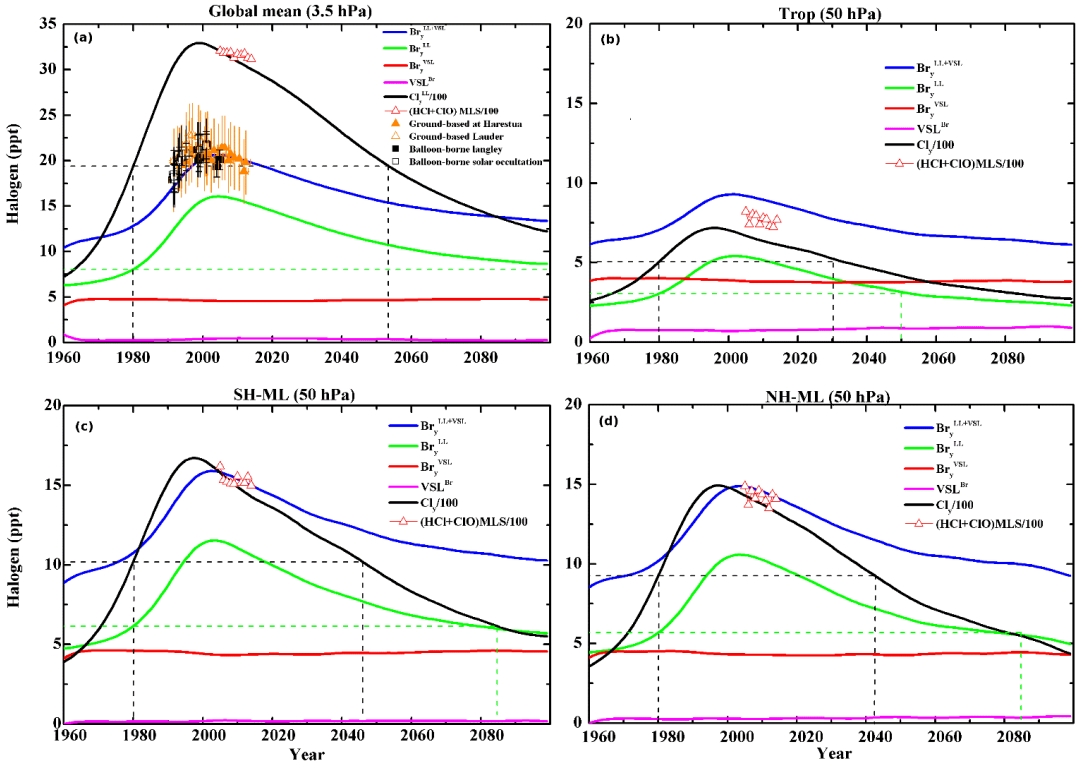


**Figure 1: Temporal evolution (1960–2100) of the modelled annual mean abundances of inorganic chlorine ($Cl_y^{LL}$) and bromine ($Br_y^{LL+VSL}$), as well as the $VSL^{Br}$ sources, in the (a) global upper stratosphere (3.5 hPa) and lower stratosphere (50 hPa) at (b) tropics, (c) SH-ML and (d) NH-ML. The $Br_y^{LL+VSL}$ abundance was split into their long-lived ($Br_y^{LL}$) and very short-lived ($Br_y^{VSL}$) contributions. The both (filled and open) black squares and (filled and open) orange triangles of the panel (a) show changes in total $Br_y$ between 1991 and 2012, derived from stratospheric BrO observations by balloon-borne (Dorf et al., 2006) and ground-based UV-visible (at Harestua (60°N) and Lauder (45°S)) measurements (Hendrick et al., 2007, 2008), respectively. The red triangles of all panels show the mean annual mixing ratios of the sum of HCl and ClO from the Microwave Limb Sounder (MLS) data (Waters et al., 2006; Livesey et al., 2018) from 2005 to 2015. The dotted horizontal lines indicate the modelled $Cl_y^{LL}$ and $Br_y^{LL}$ abundances for 1980. Note that both $Cl_y^{LL}$ values and (HCl + ClO) MLS data were divided by 100.**

https://doi.org/10.5194/acp-2019-1091
Preprint. Discussion started: 24 January 2020


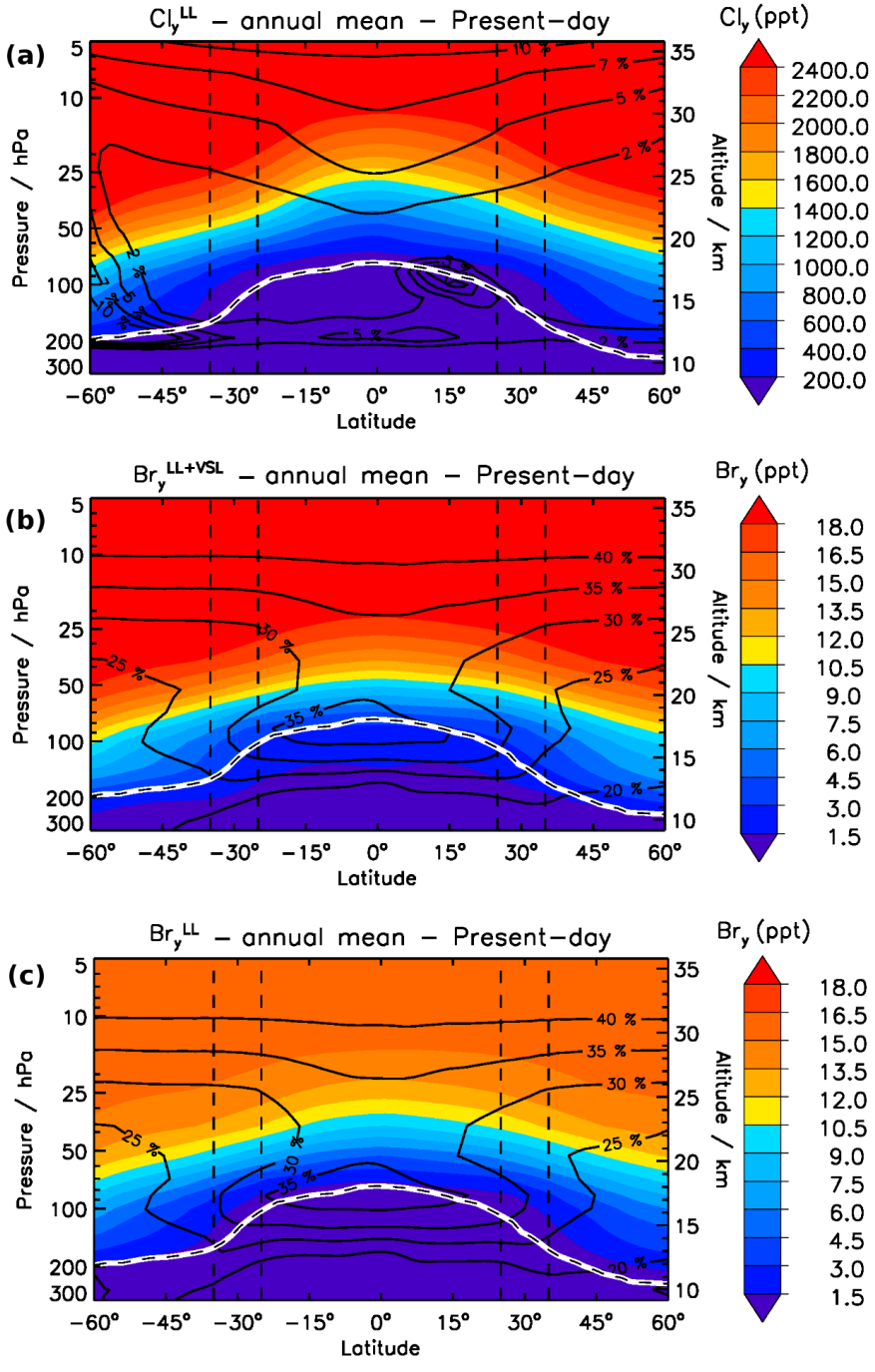


**Figure 2: Annual zonal mean distribution of (a) $Cl_y^{LL}$, (b) $Br_y^{LL+VSL}$ and (c) $Br_y^{LL}$ during the present-day period. The colour scale represents volume mixing ratios (ppt), while black contour lines show the percentage contribution of $ClO_x$ to $Cl_y$ and $BrO_x$ to $Br_y$, respectively. The lower solid white line indicates the location of the tropopause (chemical definition of 150 ppb ozone level from run$^{LL}$ experiments).**

https://doi.org/10.5194/acp-2019-1091
Preprint. Discussion started: 24 January 2020


Atmospheric Chemistry and Physics Discussions

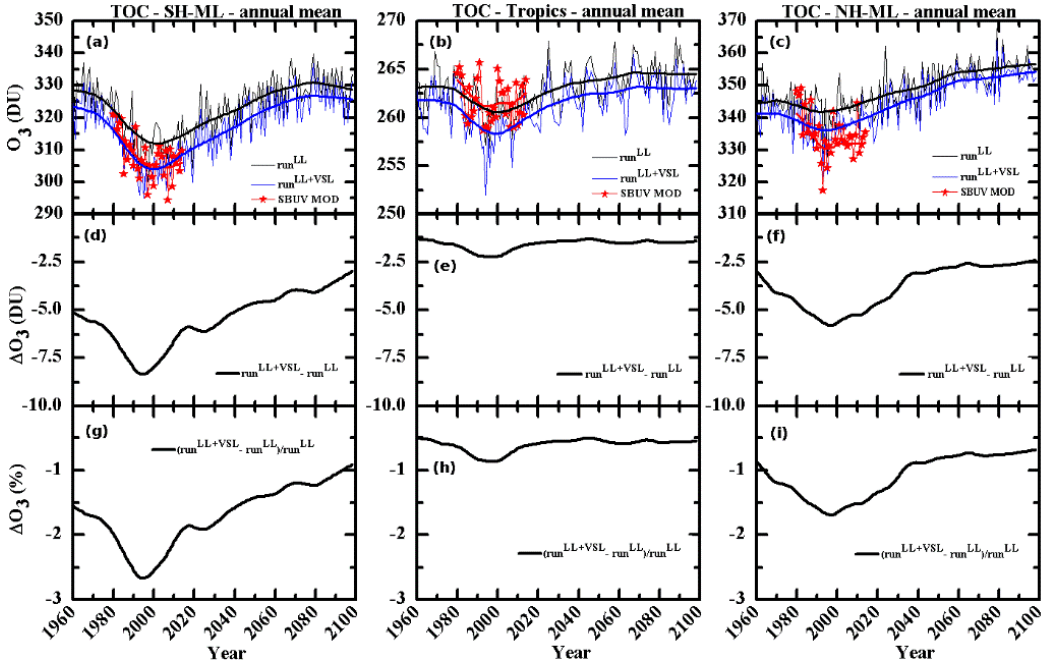


**Figure 3: Temporal evolution of the annual mean total ozone column (TOC) for the $run^{LL+VSL}$ and $run^{LL}$experiments within the (a) SH-ML, (b) tropics and (c) NH-ML, as well as the corresponding absolute (DU; d,e,f) and relative (%; g,h,i) TOC difference (ΔTOC). TOC values for the ensemble mean (thin lines) and the time-series smoothed applying a lowess filtering (0.2 fractions) (thick lines) are shown in blue for $run^{LL+VSL}$ and black for $run^{LL}$. The red lines and symbols show the observations from the Solar Backscatter Ultraviolet (SBUV) merged total ozone column data set (Waters et al., 2006; Livesey et al., 2018), within the same spatial and temporal mask as the model output.**

https://doi.org/10.5194/acp-2019-1091
Preprint. Discussion started: 24 January 2020


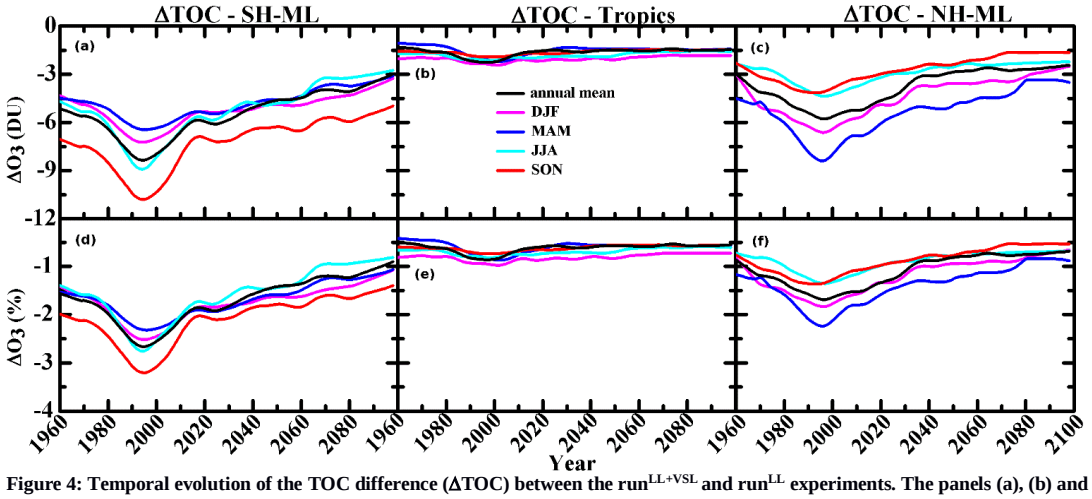


**Figure 4: Temporal evolution of the TOC difference (ΔTOC) between the run$^{LL+VSL}$ and run$^{LL}$ experiments. The panels (a), (b) and (c) show the annual and seasonal mean absolute ΔTOC (DU) within the SH-ML, tropics and NH-ML, respectively, while the panels (d), (e) and (f) show the corresponding relative ΔTOC (%).**

https://doi.org/10.5194/acp-2019-1091
Preprint. Discussion started: 24 January 2020


Atmospheric Chemistry and Physics Discussions

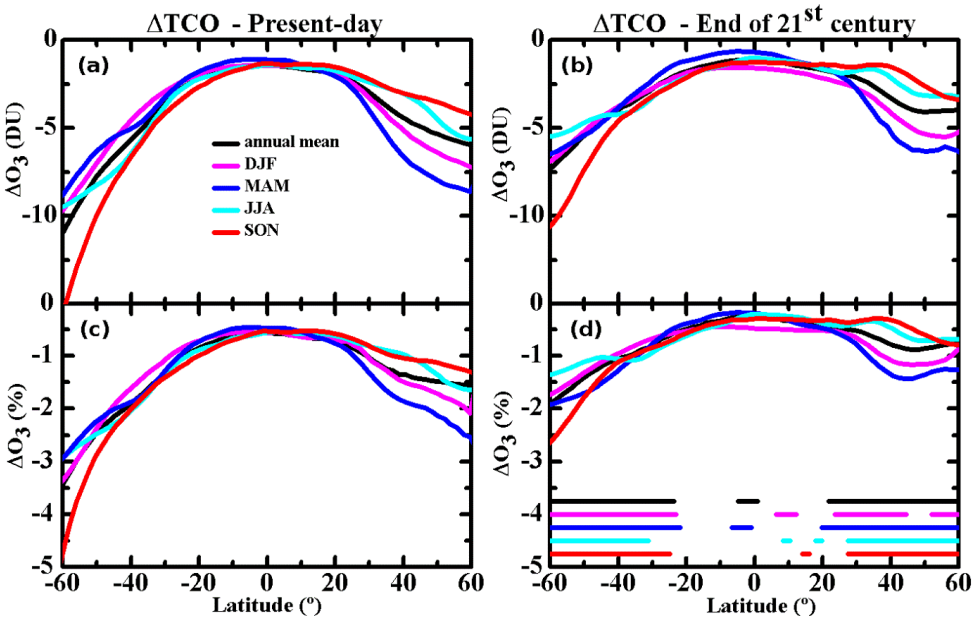


**Figure 5: Latitude distributions of ΔTOC between the experiments. The panels (a) and (b) show the annual and seasonal mean absolute ΔTOC (DU) for the present-day and the end of 21st century periods, respectively, while the panels (c) and (d) show the corresponding relative ΔTOC (%). The corresponding horizontal lines shown in the panel (d) indicate where the relative ΔTOC between the present-day and the end of the 21st century periods are statistically significant, at the 95% confidence interval using a two-tailed Student's *t* test.**

https://doi.org/10.5194/acp-2019-1091
Preprint. Discussion started: 24 January 2020


Atmospheric Chemistry and Physics Discussions

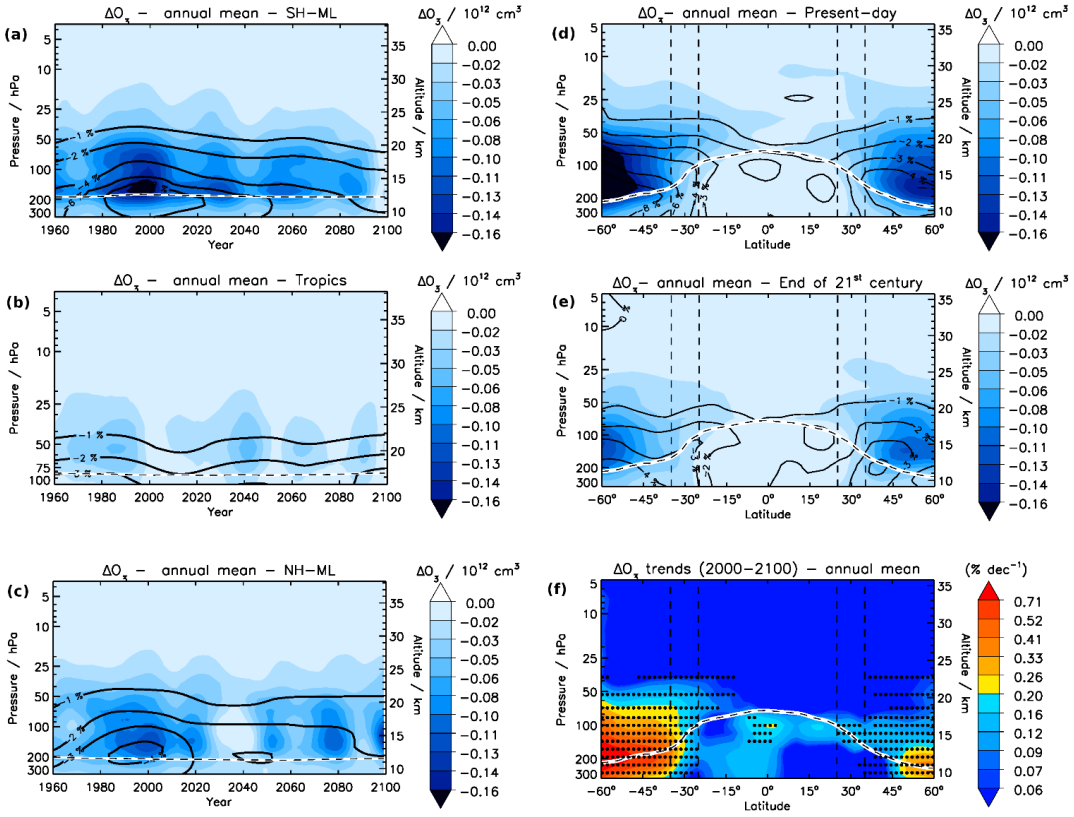


**Figure 6: Temporal evolution of the annual mean ozone ($\Delta O_3$) difference between experiments as a function of altitude, within of (a) SH-ML, (b) tropics and (c) NH-ML. The right panels shows the zonal mean $\Delta O_3$ distributions for the (d) present-day and (e) the end of the 21st century periods, as well as the (f) $\Delta O_3$ trends (% dec$^{-1}$) over the century. The absolute (colour scale) and relative (contour line) ozone differences were calculated considering the ozone number densities (i.e. molecule cm$^{-3}$) of each experiments. The masked regions in the panel (f) indicate where the relative $\Delta O_3(z)$ between the present-day and the end of the 21st century periods are statistically significant, at the 95% confidence interval using a two-tailed Student's *t* test.**

https://doi.org/10.5194/acp-2019-1091
Preprint. Discussion started: 24 January 2020


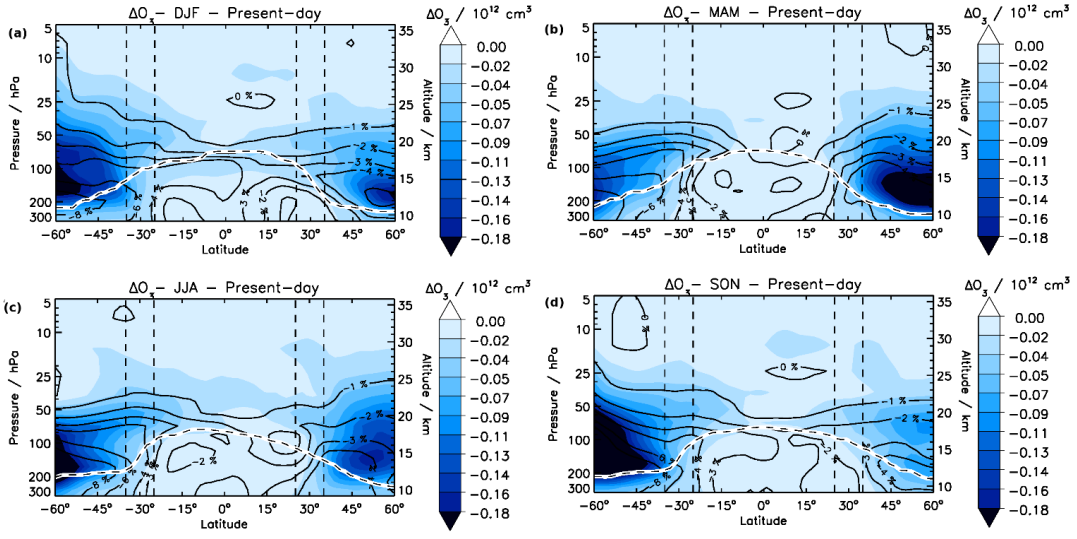


**Figure 7: Seasonal zonal mean $\Delta O_3$ distributions for the present-day period.**

https://doi.org/10.5194/acp-2019-1091
Preprint. Discussion started: 24 January 2020


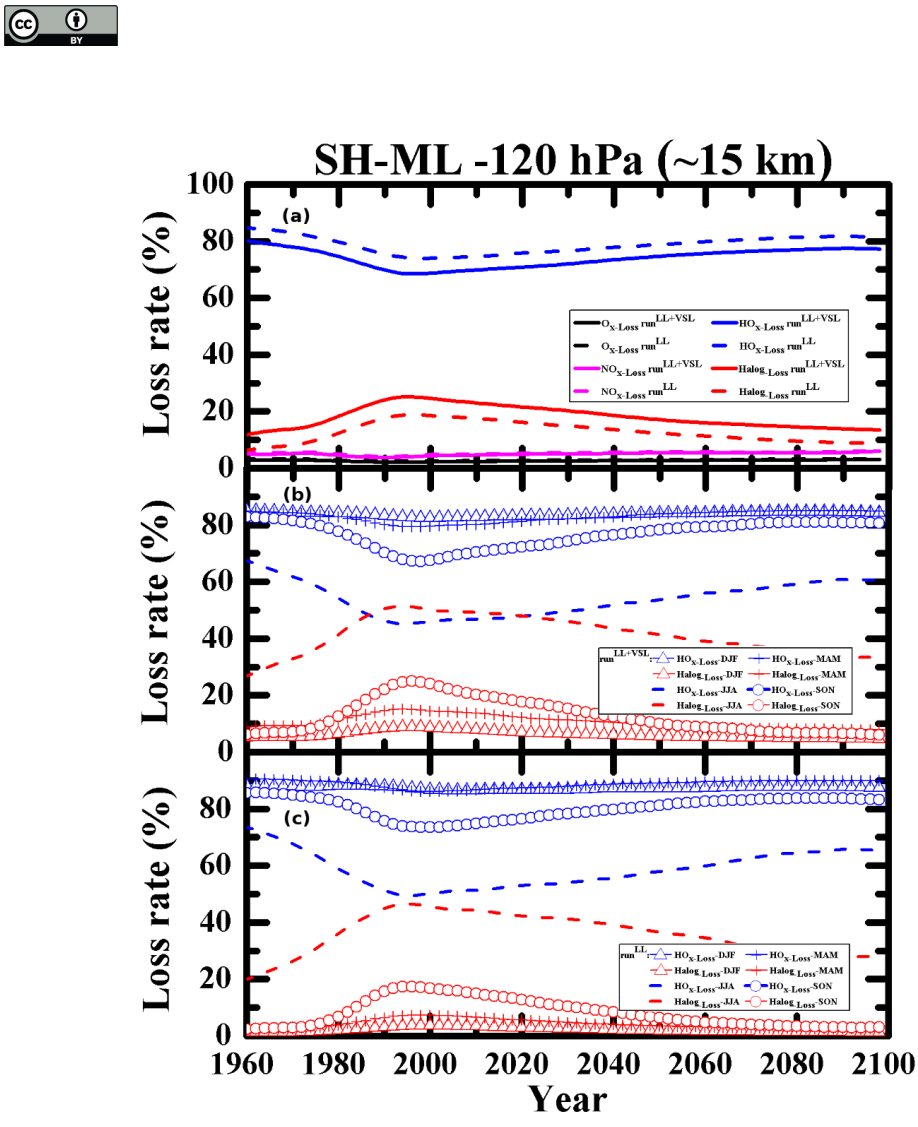


**Figure 8: Temporal evolution of the percentage contributions from ozone-depleting families ($O_{x-Loss}$, $HO_{x-Loss}$, $NO_{x-Loss}$ and $Halog_{-Loss}$) to the total odd-oxygen loss rate, over the SH-ML lowermost stratosphere (120 hPa). The panel (a) shows the annual mean contribution of each ozone-depleting family for the $run^{LL+VSL}$ (solid line) and $run^{LL}$ (dashed line) experiments. The panels (b) and (c) show the seasonal mean contributions of the $HO_{x-Loss}$ and $Halog_{-Loss}$ families for the $run^{LL+VSL}$ and $run^{LL}$ experiments, respectively.**

https://doi.org/10.5194/acp-2019-1091
Preprint. Discussion started: 24 January 2020


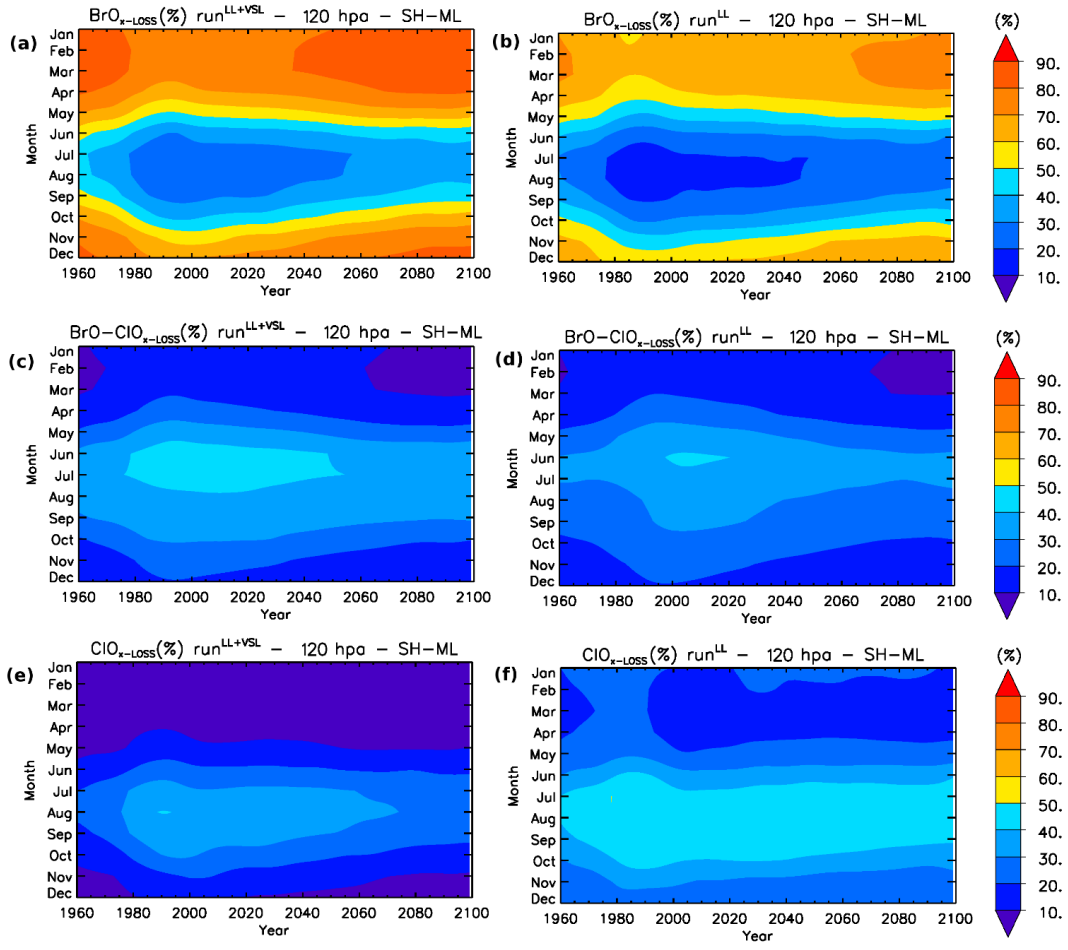


**Figure 9: Evolution of the (a,b) $BrO_{x-Loss}$, (c,d) $ClO_x$–$BrO_{x-Loss}$ and (e,f) $ClO_{x-Loss}$ percentage contributions to $Halog_{-Loss}$ as a function of the year and month, over the SH-ML lowermost stratosphere (120 hPa). The left panels show the result for $run^{LL+VSL}$ experiments, while the right panels show result for $run^{LL}$experiments.**